Mediterranean Extreme Precipitation: Amplification by Warmer Sea Surface Temperatures in a Kilometer-Scale Regional Model

Margot Bador, Julien Boé, Cécile Caillaud, Laurent Terray, Marie-Pierre Moine, Antoinette Alias

▶ **To cite this version:**

Margot Bador, Julien Boé, Cécile Caillaud, Laurent Terray, Marie-Pierre Moine, et al.. Mediterranean Extreme Precipitation: Amplification by Warmer Sea Surface Temperatures in a Kilometer-Scale Regional Model. 2024. hal-04417064

HAL Id: hal-04417064
https://hal.science/hal-04417064

Preprint submitted on 25 Jan 2024

HAL is a multi-disciplinary open access archive for the deposit and dissemination of scientific research documents, whether they are published or not. The documents may come from teaching and research institutions in France or abroad, or from public or private research centers.

L'archive ouverte pluridisciplinaire **HAL**, est destinée au dépôt et à la diffusion de documents scientifiques de niveau recherche, publiés ou non, émanant des établissements d'enseignement et de recherche français ou étrangers, des laboratoires publics ou privés.

Mediterranean Extreme Precipitation: Amplification by Warmer Sea Surface Temperatures in a Kilometer-Scale Regional Model

Margot Bador[1,*], Julien Boé[1], Cécile Caillaud[2], Laurent Terray[1], Marie-Pierre Moine[1], Antoinette Alias[2]

[1] CECI, Université de Toulouse, CERFACS/CNRS, Toulouse, France
[2] CNRM, Université de Toulouse, Météo-France, CNRS, Toulouse, France

[*] corresponding author: bador@cerfacs.fr

ORCIDs:
Margot Bador: 0000-0003-3976-6946
Julien Boé: 0000-0003-2965-4721
Cécile Caillaud: 0000-0003-2317-4129
Laurent Terray: 0000-0001-5512-7074
Marie-Pierre Moine: 0000-0002-6618-7782
Antoinette Alias: 0000-0002-8886-2830

Abstract

We employ convection-permitting regional climate modeling to analyze the intense Mediterranean Heavy Precipitation Event (HPE) in October 2020 in the south-eastern French Alps and north-western Italian Alps regions, post passage of extra-tropical storm Alex. Exploring the event's sensitivity to warmer sea surface temperatures (SSTs), we conduct modeling experiments for September-October 2020 in western Europe. An ensemble-based approach is adopted to comprehensively assess local uncertainties purely driven by internal variability.

Using the CNRM-AROME model, we accurately reproduce the HPE and precursor storm Alex characteristics, including the observed sequence of extreme events and related regional to local impacts. Sensitivity experiments are then conducted with idealized and uniform 2K warming and cooling patterns added to the SSTs over the entire domain and the Mediterranean Sea solely, all other forcings kept identical and representative of the 2020 observed conditions.

SST warming intensifies the HPE's extremeness and accumulated precipitation amounts over the Alps. This is accompanied by a shift of the most intense precipitation eastward. In contrast, the strengthening of storm Alex with SST warming has limited impact on the Mediterranean HPE. Our findings underscore the crucial role of Mediterranean warming, enhancing moisture and instability upstream, and fostering deep atmospheric convection over the mountainous coastal region. A plausible worst-case scenario testing warmer SSTs in 2022 on HPE and storm Alex suggests milder precipitation-related impacts in the French Alpes-Maritimes region but increased damage in Italy.

Keywords

Heavy precipitation events; intensification of extreme precipitation; sensitivity to sea surface temperature; kilometer-scale regional climate modeling; convection-permitting modeling

1. Introduction

On the 1st of October 2020, the intense extra-tropical storm Alex hit the north-west coasts of France, bringing heavy rainfall, and causing flooding and damage to the electricity network (Kreitz, 2021). Very intense wind gusts of remarkable intensity for this time of year were recorded. Around the low-pressure system centered at the tip of Brittany, a rapid southerly flow of warm and moist air triggered a very wet disturbance over a large part of eastern France.

Local strengthening of convective precipitation due to orographic lifting and low-level wind convergences, along with slow-evolving large-scale situation, led to record-breaking rainfall amounts over the 2nd and the 3rd of October in south-eastern French Alps and north-western Italian Alps regions. More than 600mm in 24 hours and 90mm in 1 hour were recorded in the French Alpes-Maritimes region (Chochon et al., 2021; Kreitz, 2021; Payrastre et al., 2022). In France, this Heavy Precipitation Event (HPE) caused severe flooding and landslides, killing at least 10 people, and leaving hundreds of people homeless(Météo-France, 2021). It accounted for an economic loss of approximately 1 billion euros in damage. Several villages in the French Vésubie and Roya valleys have been isolated and without drinking water for several months due to the destruction of roads, bridges, and tunnels.

The synoptic situation of this event is typical of those observed during Mediterranean HPEs (Ducrocq et al., 2008; Khodayar et al., 2016; Nuissier et al., 2008): a quasi-stationary atmospheric system is associated with a low-level moist flow toward the coast, with a supply in water by evaporation of the autumnal warm Mediterranean sea surface temperatures (SSTs) and from remote tropical sources (Duffourg & Ducrocq, 2013; Krichak et al., 2015). Along the land coastline, heavy precipitation is triggered by local reinforcement of convective precipitation by orographic lifting, and lifting induced by low-level wind convergence and cold pools (Bresson et al., 2012; Ducrocq et al., 2008).

Although this mountainous Mediterranean region has experienced other damaging HPEs in the past, the intensity of the 2020 HPE is exceptional (Payrastre et al., 2022). Rainfall accumulations were exceptional while maximum hourly rates and discharge rates were intense yet not record-breaking for the region (Payrastre et al., 2022). This observed extreme event will serve as a crucial benchmark for studying natural hydrometeorological hazards and their evolution in the context of climate change.

The high-impact HPE of October 2-3 is the focus of this study. We take a stronger emphasis on the south-eastern French region of Alpes-Maritimes than the north-western Italian Alps due to availability of high spatial and temporal resolution observations limited to France.

Contextualizing this event within the framework of ongoing regional climate change is essential for a comprehensive understanding of its distinct characteristics and exceptional nature. Over mainland France, surface air temperatures in 2020 were estimated +1,66 °C [1.41-1.90 °C] warmer with respect to the 1900-1930 period and the projected rise is of +3.8 °C [2.9-4.8 °C] by 2100 in an intermediate scenario of emission, and up to +6.7 °C [5.2- 8.2 °C] in a very high emission scenario (Ribes et al., 2022). As for extreme precipitation, changes have been detected in the observations, with an increase in the frequency and intensity of extreme precipitation events in the French Mediterranean region (Ribes et al., 2019). SSTs in the Mediterranean basin are also rising (Simon et al., 2023) and it has been

shown that warmer SSTs can significantly intensify extreme precipitation in autumn in the western Mediterranean basin (González-Alemán et al., 2023). Furthermore, a non-linear relationship between SST warming and the intensification of precipitation extremes have been found in the Black Sea coastal region (Meredith et al., 2015).

Hence, it is essential to assess the effects of contemporary and future climate change on high-impact extreme precipitation events such as the HPE observed in October 2-3, 2020. Here, we assess how idealized warm SSTs contribute to the extremeness of this observed HPE. We further explore the sensitivity to SSTs by investigating a plausible worst-case scenario where the timeline of extreme events would occur under year 2022 warmer Mediterranean SST conditions.

We utilize convection-permitting regional climate modeling with a spatial resolution of 2.5 km to achieve realistic simulation of atmospheric deep convection and its associated triggering processes. Short-duration simulations covering September-October 2020 in western Europe are conducted, employing an ensemble-based approach to thoroughly assess local uncertainties purely driven by internal variability.

Kilometer-scale modeling has demonstrated improvements in representing hourly precipitation and extremes compared to conventional regional climate models with parametrized convection (Ban et al., 2021; Berthou et al., 2020a; Lucas-Picher et al., 2023; Pichelli et al., 2021). We carry out modeling experiments with the CNRM-AROME model that has been shown to correctly reproduce the frequency and intensity of HPEs compared to observations (Caillaud et al., 2021; Fumière et al., 2020). Additionally, it compares reasonably well with other CP-RCMs over Europe (Caillaud et al., n.d.; Coppola et al., 2020).

In section 2, we introduce the model, simulation set-up, ensemble-based simulation, description of the modelling experiments, observations, and the general framework of analysis used in this study. Results are then presented in three subsections: section 3a focuses on the simulation of the observed extreme event, section 3b assesses the impact of warmer SSTs on the simulated event, and section 3c explore the worst-case scenario. Finally, a discussion of our results is provided in section 4 followed by concluding remarks in section 5.

2. Data and Methods

2.1. Data

Hourly precipitation observations at very high spatial resolution (1 km) are taken from the COMEPHORE dataset developed by Météo-France (Fumière et al., 2020). This blended product combines *in situ* data (~4000 and ~1200 rain gauges with a daily and hourly timestep, respectively) and local radar reflectivities (5 minutes timestep) (see Appendix A of Caillaud et al. (2021) for more details). It covers mainland France and Corsica, from 1997 to 2022. COMEPHORE observations have been regridded to the CNRM-AROME curvilinear grid of 2.5 km using a second-order conservative scheme.

Hourly precipitation data is also taken from the ERA5 reanalysis, on its native spatial resolution of 25 km (Hersbach et al., 2020). The objective is not to directly compare precipitation intensity between CNRM-AROME and ERA5 considering their differences in spatial resolution and representation of convective processes (parameterized in ERA5).

Instead, the timeline of the events from the passage of storm Alex to the onset of the Mediterranean HPE and related impacts with regards to precipitation are compared.

Pseudo-observations of orography at ~90m spatial resolution are taken from the Shuttle Radar Topography Mission database (https://srtm.csi.cgiar.org/) (Jarvis et al., 2008).

2.2. The convection-permitting regional climate model CNRM-AROME

CNRM-AROME is an area limited atmospheric model. It is based on the current French numerical weather prediction (NWP) system AROME used since 2008 operationally by Météo-France and that has been continuously improved over the years to gain in accuracy of prediction for extreme precipitation events and HPEs particularly (Brousseau et al., 2016; Seity et al., 2011).

CNRM-AROME can be considered as the climate counterpart to the NWP model AROME. They share the same physics and non-hydrostatic dynamical core. Apart from the use of data assimilation in the case of the NWP model, the two models differ mainly in their resolution and a wider relaxation zone for CNRM-AROME, for a stronger constrain from the driving data within the inner model (see (Caillaud et al., 2021) for more details). In addition, the NWP model AROME has been proven to accurately forecast both the extra-tropical storm ALEX and the HPE of October 2-3 in the French Alpes-Maritimes region a day before the event (Chochon et al., 2021). For all these reasons, CNRM-AROME is considered a good candidate for the simulation of this observed extreme precipitation event.

The advection scheme is semi-Lagrangian and the time discretization is semi-implicit. The bi-spectral dynamical core is non-hydrostatic, which, along with the km-scale modeling, allows the explicit simulation of the deep atmospheric convection, whereas shallow convection at the sub-grid scale still requires to be parameterized.

The physiographic contrasts (land, urban, sea and inland waters) are finely described (1km; ECOCLIMAP database; (Masson et al., 2003)) using four tiles per grid cells. Soil-atmosphere interactions are resolved by the SURFEX V8 model (Le Moigne et al., 2020; Masson et al., 2013). The version of CNRM-AROME used in this study is cycle46t1, succeeding version cycle41t1 previously evaluated specifically for Mediterranean HPEs (Caillaud et al., 2021) and for north-western Europe regional climate (Lucas-Picher et al., 2023). The main differences between these two versions are: the implementation of a correction for diurnal convection under low forcing conditions, a novel oceanic flux scheme (ECUME V6;(Belamari & Pirani, 2007)), and updated land surface model SURFEX (version 8). Overall, these two versions are very close, and we therefore refer to Table 2 of (Caillaud et al., 2021) and (Lucas-Picher et al., 2023) for technical details on the model and physical parameterizations.

2.3. Simulation set-up

The simulation domain covers western Europe centered over France (Figure 1a). It has a spatial resolution of 2.5 km, with a conformal-Lambert projection, and 60 vertical levels with hybrid coordinates levels (from 10m to ~1hPa). Out of the 60 levels, 21 are under 2000m and the lower troposphere is hence finely represented in CNRM-AROME. The timestep of CNRM-AROME is 60 seconds.

Lateral Boundary Conditions (LBCs) are imposed every hour and are derived from the ERA5 reanalysis (Hersbach et al., 2020). For more details on the relaxation zone and more generally on how LBCs forcings are imposed within this spectral model, please refer to (Caillaud et al., 2021; Lucas-Picher et al., 2023).

For availability reason, the LBCs forcing data from ERA5 were taken at a lower resolution (50km) than its native resolution. In our configuration, this leads with a resolution jump of a factor 20 between the driving data and the inner model. We acknowledge this resolution jump by considering a spatial spin-up, i.e. we exclude the edges of our simulations from our analyses. This allows small scales features to fully develop away from the LBCs. Following the guidelines of (Matte et al., 2017) and previous studies (Berthou et al., 2020b; Caillaud et al., 2021; Fumière et al., 2020), we consider a spatial spin-up of 120 grid cells width. Analyses performed in this study always exclude these border areas too close to the LBCs (see Figure 1a and note that simulated data used on Figure 3 and 4 is masked according to the observational coverage which excludes grid cells within the spatial-spin up area except for a few points at the north tip of France).

SSTs are also derived from ERA5 and are imposed monthly, using 3-month centered mean. Hence, SSTs forcings in September and October consist of the August-September-October (ASO) and September-October-November (SON) mean, respectively.

Except for water vapor that is directly simulated by the model, greenhouse gases concentrations of year 2020 are taken from the Representative Concentration Pathways 4.5 (RCP4.5)(van Vuuren et al., 2011) for CO_2, N_20, CH_4, CFC11 and CFC12. Aerosols are taken from a blended product of remote sensed and simulated data (Nabat et al., 2013), providing evolutive bidimensional distributions of dust, sea salt, sulfates, and organic and black carbon aerosols.

2.4. Description of the modeling experiments

We carry out five 20-member ensembles of 2-month simulations starting on September 1st up to October 31st, 2020. All the simulations of an ensemble share the same initial conditions, which consist of the first LBC given to the entire domain for the atmosphere. All 20 ensemble members also have identical lateral and surface conditions. A very small random offset (~10^{-4} ppm) is added to the initial CO_2 concentration to each ensemble member (as in (Bador et al., 2017)), which is enough to generate differences across the simulations thanks to simulated internal variability within CNRM-AROME.

The *CTRL* experiment is the reference simulation, i.e. SSTs imposed as forcings are those of year 2020 from the ERA5 reanalysis. Then, to assess the role of warmer (and cooler) SSTs on the Mediterranean HPE of October 2-3, we conduct 4 different sensitivity tests by modifying the SSTs but keeping the initial, lateral, and surface conditions consistent and representative of September-October 2020.

A theoretical and spatially homogeneous pattern of +2°C/-2°C warming/cooling is added on the SSTs of 2020 over the whole domain (*SST+2K* and *SST-2K* experiments, respectively). These sensitivity tests are further complemented by another experiment where we add the +2°C warming pattern but restricted to a Mediterranean box [3°W-12.2°W;38°N-44.5°N] (*SST_MED+2K* experiment; see box on Figure 2).

We realize another experiment where SSTs of 2022 are used as surface forcings instead of those of 2020 (*SST2022* experiment). The motivation behind this is that SSTs during summer 2022 were anomalously hot (between +1.3 °C and 2.6 °C compared to 1982–2011; Guinaldo et al., 2023) due to record-breaking marine heatwaves during summer in the Mediterranean basin (González-Alemán et al., 2023; Guinaldo et al., 2023) that led to warmer SSTs in fall 2022 compared to 2020 (Supplementary Figure 1). Years 2020 and 2022 are sufficiently close in time so that we can assume the observed extreme rainfall event of 2020 could have occurred in 2022, and that warming trends are of reasonable similarity between these two years. This last modeling experiments thus allows exploring the plausible worst-case scenario of the observed extreme events in 2020 (i.e. its synoptic conditions) occurring only two years later in 2020 under warmer SSTs conditions.

According to ERA5 reanalysis data, the 2020 seasonal mean ASO and SON SSTs over the whole domain are very close to the 1993-2022 climatology (Figure 2, first column). SSTs are much warmer in 2022 (González-Alemán et al., 2023), with anomalies higher than 2°C in the Mediterranean basin (Figure 2, second column). These 2022 SST anomalies in the center of the Mediterranean box are close but slightly lower than the theoretical *SST+2K* ones, whereas in the Atlantic Ocean for instance, SSTs in 2022 are generally cooler (at least 1°C) than the idealized *SST+2K* (Figure 2, third column). Finally, *SST-2K* temperatures are much cooler than the 1993-2022 climatology (between -0.5°C and -2.5; Figure 2, last column).

2.5. General framework of analysis

The majority of the analyses are performed over three different domains: the entire domain (Figure 2a), an intermediate domain covering the western Alps ([5°W-10°W;43.5°N-47.5°N], larger box on Figure 2a), and a smaller region centered over the French Alpes-Maritimes region that was heavily impacted by the 2020 Mediterranean HPE (6.6°W-8°W;43.5°N-44.6°N, smaller box in Figure 2a). Comparisons between the observations and the model are limited by the spatial coverage of COMEPHORE (France and Corsica Island; Figure 3).

Throughout this work, emphasis is given on the 5-day window centered on October 2 (i.e. September 30 to October 4), especially when focusing on the evolution of precipitation at the hourly scale. This time window also captures the Alex storm hitting the coast of France on October 1.

3. Results

3.1. Simulation of the observed extreme precipitation event

In this section, we demonstrate that the *CTRL* ensemble of CNRM-AROME simulates reasonably well the observed Mediterranean HPE of October 2-3. Our primary objective here is not to strive for the most realistic simulation of the observed event, a goal that could have been pursued through spatial resolution refinement and additional model tuning. Instead, we aim to replicate the general features of the HPE and the sequence of the precipitation events that unfolded in the first days of October 2020, along with the full distribution of outcomes due to internal variability.

First, we show that the ERA5 reanalysis captures well the sequence and the exceptional intensity of the observed extreme precipitation event (Figure 3, first two columns). Hence, using ERA5 as forcings to CNRM-AROME is relevant for the purpose of this study.

Extra-tropical storm Alex hits Brittany on October 1, bringing heavy rainfall over this area and the western part of France more generally (Figure 3, left). The Mediterranean HPE in the south-eastern French Alps and north-western Italian Alps then occurs on October 2 with intense precipitation recorded. The peak of the event is at 20:00 GMT +1 in ERA5 and 18:00 GMT +1 in COMEPHORE in the evening of October 2, showing a reasonable alignment between the two.

In addition, both the reanalysis and observations indicate relatively similar level exceedances for the HPE intensity based on their respective 5-day climatology (September 30 to October 4; 1993-2022 for ERA5, 1997-2022 for COMEPHORE): hourly precipitation rates exceed approximately 5 times the climatological values across their respective full domain, around 10 times for an intermediate domain representative of the eastern Alps region, and roughly 50 times for the core region of the French Alpes-Maritimes region (which extends over Italy in ERA5; Figure 3 first two columns).

Then, we evaluate precipitation simulated by the CP-RCM CNRM-AROME. On average over the observational domain (France and Corsica), the evolution of hourly precipitation from September 30 to October 4 compares well between COMEPHORE observations and the *CTRL* ensemble mean (Figure 3b,c).

Focusing on the French Alpes-Maritimes region affected by the intense Mediterranean HPE, we find that COMEPHORE presents four organized bands of heavy rainfall tilted along the south-west to north-east direction. These “rainfall corridors” are mainly located over the valleys (Figure 1, top; Figure 3, second column). Locally, several valleys are oriented along the axis of the low-level flow, causing air parcels to lift abruptly when encountering pronounced contrasts in terrain. Hence, orographic lifting, coupled with the stationary nature of the triggering zones, resulted in convective cells consistently forming in nearly the same locations, where significant accumulations of precipitation were observed (Chochon et al., 2021; Kreitz, 2021).

These rainfall bands are not found in the *CTRL* ensemble mean (Figure 3, third column). Valleys are represented in CNRM-AROME, but the orography contrasts appear smoother compared to observations (Figure 1), potentially contributing to certain simulated precipitation biases. CNRM-AROME tends to precipitate over larger areas in the south-east of France and the core region of the Alpes-Maritimes. It also underestimates the highest intensities when compared to the observations (Figure 3e,f and 3h,i). At the center of the observed heavy rainfall bands, where intensities are the highest, hourly precipitation accumulated over the 24-hour window that best captures the Mediterranean HPE (i.e. October 2 at 5am to October 3 at 4am) exceed 500 mm in the observations, contrasting with 350 mm in CNRM-AROME.

Hence, on average over the French Alpes-Maritimes region, hourly precipitation rates compare relatively well between the observations and CNRM-AROME. This hides a compensatory effect, where the model captures a larger area impacted by heavy rainfall, but the observations exhibit higher intensities (Figure 3 and Supplementary Figure 2 for maps of bias). The model’s overestimation of the area affected by intense hourly rainfall leads to higher peak intensities in the precipitation distribution compared to the

observations averaged over the intermediate domain of the western Alps and the French Alpes-Maritimes region (Figure 3).

We further evaluate simulated precipitation with regards to hourly precipitation extremes. Daily maximum values of hourly precipitation over the 2-month duration of the *CTRL* simulation are compared to the observations, on average over the three domains (Figure 4). October 2 exhibits the highest values in both the model and the observations, for the three different domains but the smaller domain of the French Alpes-Maritimes region more particularly. Daily maximum of hourly precipitation on October 2 is therefore taken as an indicator of extremeness of the observed Mediterranean HPE and is further investigated throughout this work.

As previously noted, we find higher intensities during the HPE when spatially averaged in *CTRL* ensemble mean compared to the observations, for the three regions considered. This pattern is consistently replicated in all 20 members of *CTRL*, which exhibit a relatively uniform simulation of the hourly evolution of spatially averaged precipitation (Supplementary Figures 2). None of the ensemble members can reproduce the observed rainy bands and the observed pronounced spatial contrast in accumulated precipitation amounts (Supplementary Figure 3).

Interestingly, the largest spread in average precipitation among the 20 members of *CTRL* is not found on October 2 despite the HPE occurrence (Figure 4), which tends to indicate a strong dynamical control by the synoptic situation. Throughout the simulation, bursts of simulated internal variability occur on specific days (e.g., September 19-24), while on other days, inter-member differences are limited (e.g. October 25 has larger precipitation than September 19-24 yet smaller inter-member differences; Figure 4). These bursts of simulated internal variability are also evident at the hourly scale during the HPE (Supplementary Figure 2). Similar to the daily scale, the highest inter-member differences do not coincide with the peak of the event but rather with its onset. Overall, all 20 members of *CTRL* compare reasonably well with the observations over the 2-month simulation period concerning daily maxima of hourly rainfall (Figure 4). All members replicate the observed Mediterranean HPE with a similar pattern (Supplementary Figures 2 and 3), although some inter-member differences capturing some stochasticity.

We argue that the ensemble-based simulation is important for case studies of extreme precipitation to fully capture an event, including the most extreme rainfall intensities that can be reached locally. These stochastic differences purely driven by internal variability lead to different impacts locally, justifying the need to fully consider them in our simulations. Indeed, the km-scale modelling allows the production of relevant local climate information, which should always be associated with its relevant uncertainties.

This is demonstrated using the maximum values of hourly precipitation on October 2 as a measure of extremeness that we compare along the different realizations of the *CTRL* ensemble. Inter-member spread is the highest over the ocean and in the eastern part of simulation domain (Figure 5b,c). Focusing regionally on the intermediate domain of the western Alps, it becomes evident that each of the 20 members exhibits slightly different spatial distributions of the extreme rainfall cells (Figure 5d-w). Particularly in Italy, the highest intensities can be found further eastward or northward according to the members.

3.2. Impact of 2°C warmer and cooler SSTs on the simulated extreme precipitation event

In this section, we explore the sensitivity of extreme precipitation to different SST conditions. Taking the *CTRL* ensemble as the reference, we assess the response of hourly precipitation in the modelling experiments where SSTs forcing conditions are modified using idealized patterns of uniform 2K warming and cooling. A plausible worst-case scenario with the observed SSTs of 2022 and related response in extreme precipitation will be discussed in the next section.

First, we explore the role of SSTs on the extremeness of precipitation throughout the 2-month duration of the simulations. On average over the entire domain, daily maxima of hourly precipitation generally respond as follow: 2K cooler SSTs lead to lower intensities (*SST-2K* experiment; blue line; Figure 6a) compared to CTRL (black line), and 2K warmer SSTs lead to higher intensities (*SST+2K* experiment; red line). The response in *SST_MED+2K* experiment (purple line; Figure 6) shows a similar pattern with higher intensities compared to *CTRL*. However, this intensification is more moderate than in *SST+2K*. This response to warmer and cooler SSTs is less clear when averaging over the intermediate and smaller regions (Figure 6b,c). This can be expected, as thermodynamic control exerts less influence on smaller scales, whereas, conversely, dynamical processes impose stronger constraints on precipitation (Emori & Brown, 2005; Pfahl et al., 2017).

This simple extremeness measure clearly shows that hourly precipitation on October 2 can be intensified by warmer SSTs (Figure 6). We further explore the changes in the spatial distribution of hourly precipitation maxima on that day corresponding to the peak of the Mediterranean HPE in the French Alpes-Maritimes region. Locally, hourly precipitation rates higher than 60 mm are found in the *CTRL* multi-member mean, and up to 80 mm across the different ensemble members (Figure 7a versus 7b).

Warming SSTs by 2K over the entire domain leads to an eastward shift of the most intense daily maxima of hourly precipitation, with values exceeding 50 mm displaced from the French Alpes-Maritimes region towards Italy (Figure 7c; see also Supplementary Figure 4c). Interestingly, our sensitivity modeling experiments demonstrate that the warming in the western Mediterranean basin is primarily responsible for this eastward shift (Figure 7d). Indeed, the spatial differences between *SST+2K* and *CTRL,* and those between *SST_MED+2K* and *CTRL* are rather similar in the multi-member mean. This shows that the 2020 Mediterranean HPE is highly sensitive to regional SSTs. In contrast, cooling SSTs by 2K over the entire domain leads to a decrease in the area affected by heavy precipitation compared to *CTRL* and lower intensities of daily maxima (Figure 7f), except for the north-western corner of Italy, where maxima are more intense in *SST-2K* (Supplementary Figure 4f).

Generally, a similar response is found for the evolution of hourly precipitation on average over the entire domain: warmer SSTs lead to an intensification of precipitation throughout the HPE duration, whereas cooler SSTs lead to a decrease in intensity (Figure 8a). Over the intermediate domain of the western Alps, the response of hourly precipitation to SSTs is very similar but the HPE tends to be shifted in time by a couple of hours in the *SST-2K* ensemble. Overall, the hourly evolution of average precipitation compares well between the *SST+2K* and *SST_MED+2K*, especially during the HPE and over the Alps region. This once again emphasizes that the HPE intensity is sensitive to regional SSTs.

Over the smaller domain of the French Alpes-Maritimes region, it his harder to extract general conclusions on the sensitivity of hourly precipitation to warmer and cooler SSTs (Figure 8c). The initiation of the HPE in the early hours of October 2 experiences a delayed onset by a few hours under warmer SSTs compared to colder SSTs. Hourly precipitation rates tend to be higher in *SST_MED+2K* compared to *SST+2K* but not consistently throughout the HPE. In addition, hourly precipitation averaged over this smaller domain does not consistently exhibit an intensification with warmer SSTs compared to *CTRL*. This contrasts with the general increase on average over the larger domain where the thermodynamic control is stronger. The interpretation of the response to SST warning is here limited by the blending of spatially contrasting responses explored hereafter.

The spatial distribution of accumulated precipitation over the 24h hours period that best represents the duration of the HPE (grey shading on Figure 8) depicts a similar eastward shift of the precipitation areas with warmer SSTs (Figure 9; see also Supplementary Figure 5). This aligns with the changes in daily maxima of hourly precipitation (Figure 7). We note once again that SST warming solely in the western Mediterranean basin leads to a very similar response in accumulated precipitation (Figure 9b,c). However, the decrease in intensity over the French Alpes-Maritimes region is slightly smaller in *SST_MED+2K* compared to *SST+2K*, while the intensification is more pronounced in *SST_MED+2K* in Italy (Figure 9b,c). The impact of cooler SSTs on accumulated precipitation amounts is also in general agreement with results on daily maxima of hourly precipitation (Figure 9e). A decrease in intensity is found in the area with the highest rainfall *CTRL*, while an intensification occurs in the north-wester corner of the Italian Alps (Figure 9e).

One strength of our modeling study lies in our ability to simulate the entire sequence of events that led to the occurrence of the Mediterranean HPE in the south-eastern French Alps and the north-western Italian Alps on October 2-3, covering a substantial geographic domain. This allows to assess the impact of warmer (and cooler) SSTs on the extra-tropical storm Alex, how this can further induce modifications on the synoptic forcings responsible for the onset of the HPE, and the consequences at the local scale of the French Alpes-Maritimes region. Our focus hereafter is on the 24h period that best captures the HPE, from October 2 at 5am to October 3 at 4am (grey shadings on Figures 3 and 8).

In the *CTRL* ensemble, we find that low pressures associated with the extra-tropical storm Alex are located at the west tip of France (Britany region), with minimum values of 980.5 hPa in the core of the system (Figure 10a). Around the low pressures, strong onshore winds bring maximum near-surface wind speed of gusts exceeding 150 km/h over the west coast of France and Britany (i.e. maximum values over the 24h period and across the 20 members; Figure 11a). The location of storm Alex over Britany induces a south-eastern flow in eastern side of the western Mediterranean basin, a rapid southern flow in the center of the basin, and a south-western flow on the western side. These low-level flows are heading towards the orographic barrier of the southern French and Italian Alps (Figure 10a).

Warming SSTs of 2K over the entire simulation domain leads to lower minimal values of sea level pressure at the center of the low-pressure system (978.8 hPa in *SST+2K*; Figure 10b) whereas SST cooling results in higher values (980.6 hPa in *SST-2K*; Figure 10e). Moreover, warmer SSTs contribute to an expanded spatial extent of low sea-level pressures, while cooler SSTs result in a reduction. Over the west coast of France, this has a clear impact on wind gusts with amplification and attenuation depending on the positive or negative SST

anomalies (Figure 11b,e). Overall, we find that warming (cooling) the SST consistently leads to a negative (positive) response in sea level pressure, over both the Atlantic Ocean and the Mediterranean Sea (Supplementary Figure 6).

Focusing on the *SST_MED+2K* ensemble, we find that the spatial extent of the low-pressure system and the maximum wind gust intensities generally resemble those in *CTRL* (Figure 10c and Figure 11c). This alignment is anticipated, considering that SSTs remain unaltered over the Atlantic Ocean in this modeling experiment. Interestingly, patterns of sea level pressure change compare well between *SST+2K* and *SST_MED+2K* in the western Mediterranean Sea region. This indicates that changes in the characteristics of extra-tropical storm Alex have limited impact on the changes in regional atmospheric circulation over the Mediterranean Sea. These changes are primarily controlled by the response to regional sea surface warming.

In both *SST+2K* and *SST_MED+2K* experiments, a negative response in sea level pressure leads to wind anomalies circumventing the north of Corsica (Supplementary Figure 6b,c). This results in a tilting of the atmospheric flow in the eastern side of the simulated Mediterranean domain, with a direction that becomes less southerly and more south-southeasterly oriented. Meanwhile, in the western side, the low-level flow weakens and penetrates less deeply inland into Italy compared to *CTRL* (Figure 10 and Supplementary Figure 6).

Finally, we investigate the mechanisms responsible for the changes in accumulated precipitation with warmer (and colder) SSTs over the south-eastern French Alps and north-western Italian Alps over the 24h period of the Mediterranean HPE (Figure 12, first row).

Regionally, warmer SSTs lead to heating in the near-surface troposphere (Figure 12, second line). In turn, an increase in specific humidity is associated with the surface heating (Figure 12, third row). Changes in moisture convergence across the different modeling experiments helps understanding some of the changes in accumulated precipitation. Indeed, in *SST+2K*, moister air is advected further eastward to the French Alpes-Maritime region. Similarly, in Italy, weaken atmospheric flow with increased moisture leads to higher accumulations eastward (i.e. upstream) to the region the most affected in *CTRL* (Figure 12, first row). In contrast, the cold SST experiment is associated with decreased moisture converging onshore and generally lower accumulations in precipitation, except for north-western Italy, where stronger westward winds bring moist air closer to the Alps with locally an intensification of rainfall.

These thermodynamic changes alone cannot fully explain the overall precipitation changes during the HPE. Thermodynamical changes are intertwined with dynamic changes, and while considering them separately has its limitations, it helps gaining a more comprehensive understanding of the effects induced by warming the SSTs. Generally, warmer SSTs lead to larger CAPE values and thus to increased lower tropospheric instability which is advected onshore (Figure 13, first row). Upstream instability is carried inland and is a favoring factor to trigger deep atmospheric convection. Higher in the troposphere (at 700 hPa), vertical velocities are enhanced east of the French Alpes-Maritimes region where rainfall accumulation is higher in *SST+2K* (Figure 13, second row). In addition, an increase in relative humidity is found in areas where the atmospheric conditions were not already saturated in *CTRL* (Figure 13, third row). These dynamical changes are all ingredients to enhance deep atmospheric convection, and indeed, precipitable water is increased where instability and moisture increases are collocating (Figure 13, fourth row).

We note once again that the thermodynamic and dynamic changes are generally similar in the *SST_MED+2K* and *SST+2K* experiments (Figures 12 and 13). This highlights again that the regional warming of SSTs has a crucial role on the 2020 Mediterranean HPE in amplifying the precipitation-related impacts and driving local changes.

3.3. Plausible worst-case scenario of the extreme precipitation event occurring in 2022 under warmer SSTs

The sensitivity of simulated extreme precipitation to SSTs is further assessed through a plausible worst-case scenario. We investigate how the observed Mediterranean HPE in 2020 could have been different had it occurred two years later, in 2022, under warmer SSTs conditions (Figure 2 and section 2.4). To that end, we explore the response of extreme precipitation in the *SST2022* ensemble and compare it to that of the *CTRL* experiment. Results are then contextualized with the idealized modeling experiments *SST+2K* and *SST_MED+2K*.

On average over the entire domain and over the duration of the simulations, daily maxima of hourly precipitation in *SSTs_2022* exhibit greater intensities compared to *CTRL* (green and black lines, respectively; Figure 6a). Daily maxima in *SSTs_2022* are generally close to those in *SST_MED+2K* (purple line) and generally less intense than in *SST+2K* (red line). In 2022, ASO and SON mean SST patterns closely resembles those idealized in *SST+2K* over the western Mediterranean basin (Figure 2). In contrast, over the Atlantic Ocean, SSTs in 2022 are not as anomalously warm and therefore differ from those of *SST+2K*. Thermodynamic consideration can thus broadly explain why, over the scale of the entire domain, the intensification of extreme precipitation with warmer SSTs of 2022 somehow sits in between the responses of *SST+2K* and *SST_MED+2K*. At the hourly scale throughout the Mediterranean HPE event, similar thermodynamically-driven responses are found with precipitation rates averaged over both the entire and intermediate domains of similar intensities between the *SST+2K*, *SST_MED+2K* and *SST2022* ensembles (Figure 8a,b).

Focusing on the Mediterranean HPE over the smaller region of the French Alpes-Maritimes, we find a similar response in *SST2022* compared to *SST+2K* and *SST_MED+2K* with lower daily maxima values than in CTRL on days 2, 3 and 4 of October (Figure 6c). Firstly, this reaffirms the high sensitivity of extreme precipitation in this region to regional SSTs. Then, it indicates that if storm Alex had occurred two years later, the precipitation-related impacts in the French Alpes-Maritimes region would have been less severe than those experienced in 2020. Indeed, the warmer SSTs of 2022 in the western Mediterranean basin leads to an eastward shift of the rainfall patterns. This shift is found in both the daily maxima of hourly precipitation on October 2 (Figure 7e and Supplementary Figure 4e) and the increased accumulations of precipitation (Figure 9e and Supplementary Figure 5e). In contrast, the HPE impacts would have been much more severe in Italy.

The influence of the 2022 warmer SSTs on the extra-tropical storm Alex somehow resembles a dimmed version of the response in *SST+2K*. This aligns with expectations, considering the relatively small SST anomalies in 2022 compared to 2020 in the Atlantic Ocean. A small expansion of the low-pressure system is found along with a small decrease in

minimum pressure (Figure 10d and Supplementary Figure 6d). Similarly, we find minimal impact on the maximum wind gust speeds along the western France coastline (Figure 11d).

Previous results from *SST+2K* and *SST_MED+2K* showed that changes in characteristics of storm Alex have a limited role on the Mediterranean HPE. This is confirmed with *SSTs_2022.* The response of the regional atmospheric circulation in the western Mediterranean basin resembles those in *SST_MED+2K*, albeit with slightly smaller intensity (Figure 10d and Supplementary Figure 6d). In response to warmer SST conditions in 2022, and compared to *CTRL*, a negative sea level pressure pattern leads to wind anomalies and a tilting of the low-level flow heading to the French Alpes-Maritimes region according to a south to south-easterly direction.

The thermodynamic and dynamic changes in *SST2022* are generally like those in *SST_MED+2K,* albeit with slightly lower intensities (Figures 12 and 13). Across the French Alpes-Maritimes region, these changes in thermodynamics and dynamics can generally explain the local precipitation response during the HPE. While instability is increased upstream, changes in moisture convergence between *SST2022* and *CTRL* primarily account for the decrease in extreme precipitation intensity in the French Alpes-Maritimes region. Conversely, on the other side of the Alps in Italy, changes in low-level flow, along with increased instability and moisture, contribute to more intense extreme precipitation.

4. Discussion

Hourly precipitation rates and accumulated amounts during the Mediterranean HPE simulated by CNRM-AROME compare reasonably well with high-quality observations in the French Alpes-Maritimes region. The main biases of the model lie in an underestimation of the spatial contrasts of the heavy rainfall distribution, and in an underestimation of the highest intensity, which has been previously documented in the literature (Caillaud et al., 2021; Fumière et al., 2020). Part of this bias may be attributed to the orography in CNRM-AROME, which cannot fully capture the complex spatial contrasts of this mountainous region at the 2.5 km resolution. However, this likely does not account for the entire bias.

Convective precipitation extremes are difficult to model. Furthermore, other limitations tied to the model's performance may also contribute to these difficulties. Substantial advancements have been made in recent years with convection-permitting regional climate models (CP-RCMs), particularly for hourly precipitation and extremes, compared to conventional regional climate models (Ban et al., 2021; Berthou et al., 2020b; Lucas-Picher et al., 2008; Prein et al., 2015). While CP-RCMs currently appear as our best tool to study extreme precipitation at fine spatial and temporal climate scales, ongoing model developments are essential to address the increasing demand for relevant local climate change information.

The ensemble-based modeling approach allows to assess the full range of outcomes due to internal variability, which is highly relevant to gain a better understanding of climate change impacts locally. In this study, we realized 20 simulations for each modeling experiments. All ensemble members reproduce similarly the overall sequence of observed events as they have identical large-scale forcings. However, we highlight variations locally among the ensemble members for the highest rainfall amounts locally and for the maximum near-surface wind speeds. We argue that the ensemble-based approach is important when modeling extreme events, and extreme precipitation more particularly. Impact sectors increasingly rely on the km-scale modeling to produce local climate information. This should

always be accompanied by the comprehensive description of the uncertainties, including those associated with internal variability.

Our findings consistently highlight the potential enhancement of warmer autumnal SSTs on the intensity of heavy precipitation events (HPEs) in the Mediterranean region. This is in line with previous studies that emphasize the crucial role of pre-event SST conditions in driving the intensity of such events (Berthou et al., 2014; Lebeaupin et al., 2006; Meredith et al., 2015; Rainaud et al., 2017). The onshore advection of moist and unstable air, essential for fueling convective systems during HPEs, is intricately tied to the pivotal role played by air-sea interactions in the Mediterranean Sea. These interactions contribute significantly by supplying moisture and heat to the lower atmospheric layers (Lebeaupin Brossier et al., 2008; Rainaud et al., 2017).

While investigating the impact of the air-sea interactions on the 2020 HPE case could offer valuable insights, existing studies suggest that coupled ocean-atmosphere modeling might yield significant improvements. Based on simulations involving three HPEs with consideration of coupling through air-sea interface fluxes, an oceanic response with a SST cooling under the low-level jet was identified (Lebeaupin et al., 2006). However, minimal impact was found on the 24-hour lead time forecast of heavy precipitation. The main explanation lies in the intensity of the low-level jet that leads to a forcing from the atmosphere onto the ocean during an HPE. Furthermore, the Mediterranean Sea is not the only source of moisture for feeding the convective systems. Moisture exported from the Atlantic and the Tropics contributes significantly to the amount of water vapor to supply the convection (Duffourg & Ducrocq, 2011, 2013). Our simulation domain does not encompass these moisture sources, preventing an exploration of their potential influence.

5. Conclusions

Using convection-permitting climate modeling with a spatial resolution of 2.5 km, we conduct short ensembles of 20 simulations over a period of 2 months. These simulations accurately reproduce the extra-tropical storm Alex, which initiated the development of large scale conditions favorable to the onset of an intense Mediterranean Heavy Precipitation Event (HPE). Low-level wind convergence and orographic lifting from the advection of moist and unstable air to the Alps triggered deep atmospheric convection and precipitation of rare intensity on the early days of October 2020 in the south-eastern French Alps and the north-western Italian Alps. Modeling this sequence of extreme events is a challenge. In this study, we show that the convection-permitting regional climate model (CP-RCM) CNRM-AROME can successfully reproduce such high-impact extreme precipitation events over a substantial domain.

Our main objective is to examine the role of warmer (and colder) sea surface temperatures (SSTs) in influencing the HPE intensity. We focus primarily on the effects on precipitation and in the French Alpes-Maritimes region that was severely affected by this event. We carry out three modeling sensitivity experiments, testing different SST conditions. First, idealized patterns of uniform 2K warming and cooling are applied to the 2020 SSTs over the entire domain of simulation. The influence of regional SSTs is further tested by adding 2K to the SSTS over a Mediterranean box solely.

Generally, at the scale of the simulation domain, warmer SSTs lead to an intensification of precipitation. Daily maximum values of hourly precipitation and accumulations over the course of the HPE are consistently higher under warmer SSTs conditions. The response to SST warming is more contrasted locally, which can be explained by a lesser influence of the thermodynamic change and, conversely, a stronger influence of the dynamic changes at finer spatial and temporal scales (Emori & Brown, 2005; Pfahl et al., 2017).

A key finding from our study is that the extremeness of the 2020 Mediterranean HPE can be intensified with warmer SST conditions in the western Mediterranean Sea. Extremeness is here measured by the daily maximum values of hourly precipitation on the day that received the highest rainfall. Our results indicate that the region characterized by daily maxima exceeding 60mm (in the ensemble mean) expands in simulations with warmer SSTs. The potential for precipitation amplification has also been demonstrated in the case of the 2012 Krymsk event, highlighting the influence of Black Sea surface temperatures (Meredith et al., 2015).

An additional finding is that the region affected by the most intense hourly precipitation rates are shifted eastward. This pattern is also depicted in the changes in accumulated hourly rainfall during the Mediterranean HPE. Interestingly, the eastward shift of precipitation is highly consistent in the modeling experiment with warmer SSTs imposed over the entire oceanic domain and the experiment where warming is confined solely to the Mediterranean region. This emphasizes the sensitivity of the 2020 Mediterranean HPE to regional sea surface conditions.

Over the Atlantic Ocean, SST warming leads to the deepening of the extra-tropical storm Alex and the expansion of the low pressures, in agreement with (Ginesta et al., 2023). Along the western coasts of France, wind gusts are intensified, and strong winds are simulated extending further south than under the SSTs conditions of 2020. While this storm is responsible for the development of the synoptic conditions leading to the Mediterranean HPE, our findings indicate that changes in storm Alex have limited effects on the changes in regional atmospheric circulation in the Mediterranean basin. Indeed, the regional response of the atmospheric circulation during the HPE is relatively similar between the simulations where warmer SSTs are imposed over the entire domain and over the Mediterranean region solely.

In the western Mediterranean Sea, warmer SSTs modify the low-level flow. The eastern part of the flow directed toward the French Alpes-Maritimes region tilts in a south/south-east direction under warmer SSTs, while the western part of flow weakens in intensity over inland Italy. In the lower troposphere, surface heating is associated with an increase in humidity and instability upstream, which is transported inland to the natural barriers of the Alps, where orographic lifting occurs. Deep atmospheric convection is enhanced in the modeling experiments with warmer SSTs. Overall, consideration of the thermodynamic and dynamic changes in our modeling experiments help understanding the intensification in precipitation and the eastward shift of the highest precipitation amounts with SST warming.

Finally, we explore a plausible worst-case scenario and investigate how the observed 2020 Mediterranean HPE could have been different had it occurred 2 years later, in 2022, where warmer SSTs conditions were recorded in the western Mediterranean Sea.

This worst-case scenario simulation confirms the high sensitivity of the 2020 Mediterranean HPE to regional SSTs. Furthermore, it suggests that had the extra-tropical storm Alex occurred two years later, the precipitation-related impacts in the French Alpes-Maritimes region might have been less severe than those experienced in 2020, owing to an eastward shift of precipitation. Conversely, in Italy, the potential for more significant damage would likely have increased.

Our findings demonstrate the need to further explore the effects of climate changes on extreme precipitation events in the Mediterranean region. The convection-permitting regional climate modeling appear adapted for the event-based analysis of extreme precipitation and should be further developed to explore the impacts of the future changes in the mean atmospheric circulation on extreme precipitation events locally.

References

Bador, M., Terray, L., Boé, J., Somot, S., Alias, A., Gibelin, A.-L., & Dubuisson, B. (2017). Future summer mega-heatwave and record-breaking temperatures in a warmer France climate. *Environmental Research Letters*, *12*(7). https://doi.org/10.1088/1748-9326/aa751c

Ban, N., Caillaud, C., Coppola, E., Pichelli, E., Sobolowski, S., Adinolfi, M., Ahrens, B., Alias, A., Anders, I., Bastin, S., Belušić, D., Berthou, S., Brisson, E., Cardoso, R. M., Chan, S. C., Christensen, O. B., Fernández, J., Fita, L., Frisius, T., … Zander, M. J. (2021). The first multi-model ensemble of regional climate simulations at kilometer-scale resolution, part I: evaluation of precipitation. *Climate Dynamics*, *57*(1–2), 275–302. https://doi.org/10.1007/s00382-021-05708-w

Belamari, S., & Pirani, A. (2007). *Validation of the optimal heat and momentum fluxes using the ORCA2-LIM global ocean-ice model*. Marine EnviRonment and Security for the European Area–Integrated Project (MERSEA IP), Deliverable D 4

Berthou, S., Kendon, E. J., Chan, S. C., Ban, N., Leutwyler, D., Schär, C., & Fosser, G. (2020a). Pan-European climate at convection-permitting scale: a model intercomparison study. *Climate Dynamics*, *55*(1–2), 35–59. https://doi.org/10.1007/s00382-018-4114-6

Berthou, S., Kendon, E. J., Chan, S. C., Ban, N., Leutwyler, D., Schär, C., & Fosser, G. (2020b). Pan-European climate at convection-permitting scale: a model intercomparison study. *Climate Dynamics*, *55*(1–2), 35–59. https://doi.org/10.1007/s00382-018-4114-6

Berthou, S., Mailler, S., Drobinski, P., Arsouze, T., Bastin, S., Béranger, K., & Lebeaupin-Brossier, C. (2014). Prior history of Mistral and Tramontane winds modulates heavy precipitation events in southern France. *Tellus A: Dynamic Meteorology and Oceanography*, *66*(1), 24064. https://doi.org/10.3402/tellusa.v66.24064

Bresson, E., Ducrocq, V., Nuissier, O., Ricard, D., & de Saint-Aubin, C. (2012). Idealized numerical simulations of quasi-stationary convective systems over the Northwestern Mediterranean complex terrain. *Quarterly Journal of the Royal Meteorological Society*, *138*(668), 1751–1763. https://doi.org/10.1002/qj.1911

Brousseau, P., Seity, Y., Ricard, D., & Léger, J. (2016). Improvement of the forecast of convective activity from the AROME-France system. *Quarterly Journal of the Royal Meteorological Society*, *142*(699), 2231–2243. https://doi.org/10.1002/qj.2822

Caillaud, C., Somot, S., Alias, A., Bernard-Bouissières, I., Fumière, Q., Laurantin, O., Seity, Y., & Ducrocq, V. (2021). Modelling Mediterranean heavy precipitation events at climate scale: an object-oriented evaluation of the CNRM-AROME convection-permitting regional climate model. *Climate Dynamics*, *56*(5–6), 1717–1752. https://doi.org/10.1007/s00382-020-05558-y

Caillaud, C., Somot, S., Douville, H., Alias, A., Bastin, S., Brienen, S., & et al. (n.d.). Mediterranean Heavy Precipitation Events in a warmer climate: robust versus uncertain changes with a large convection-permitting model ensemble. . *GRL (under Review)*.

Chochon, R., Martin, N., Lebourg, T., & Vidal, M. (2021, June). nalysis of extreme precipitation during the mediterranean event associated with the Alex storm in the Alpes-Maritimes: atmospheric mechanisms and resulting rainfall. *SimHydro 2021: Models for Complex and Global Water Issues*.

Coppola, E., Sobolowski, S., Pichelli, E., Raffaele, F., Ahrens, B., Anders, I., Ban, N., Bastin, S., Belda, M., Belusic, D., Caldas-Alvarez, A., Cardoso, R. M., Davolio, S., Dobler, A.,

Fernandez, J., Fita, L., Fumiere, Q., Giorgi, F., Goergen, K., … Warrach-Sagi, K. (2020). A first-of-its-kind multi-model convection permitting ensemble for investigating convective phenomena over Europe and the Mediterranean. *Climate Dynamics*, *55*(1–2), 3–34. https://doi.org/10.1007/s00382-018-4521-8

Ducrocq, V., Nuissier, O., Ricard, D., Lebeaupin, C., & Thouvenin, T. (2008). A numerical study of three catastrophic precipitating events over southern France. II: Mesoscale triggering and stationarity factors. *Quarterly Journal of the Royal Meteorological Society*, *134*(630), 131–145. https://doi.org/10.1002/qj.199

Duffourg, F., & Ducrocq, V. (2011). Origin of the moisture feeding the Heavy Precipitating Systems over Southeastern France. *Natural Hazards and Earth System Sciences*, *11*(4), 1163–1178. https://doi.org/10.5194/nhess-11-1163-2011

Duffourg, F., & Ducrocq, V. (2013). Assessment of the water supply to Mediterranean heavy precipitation: a method based on finely designed water budgets. *Atmospheric Science Letters*, *14*(3), 133–138. https://doi.org/10.1002/asl2.429

Emori, S., & Brown, S. J. (2005). Dynamic and thermodynamic changes in mean and extreme precipitation under changed climate. *Geophysical Research Letters*, *32*(17), 1–5. https://doi.org/10.1029/2005GL023272

Fumière, Q., Déqué, M., Nuissier, O., Somot, S., Alias, A., Caillaud, C., Laurantin, O., & Seity, Y. (2020). Extreme rainfall in Mediterranean France during the fall: added value of the CNRM-AROME Convection-Permitting Regional Climate Model. *Climate Dynamics*, *55*(1–2), 77–91. https://doi.org/10.1007/s00382-019-04898-8

Ginesta, M., Yiou, P., Messori, G., & Faranda, D. (2023). A methodology for attributing severe extratropical cyclones to climate change based on reanalysis data: the case study of storm Alex 2020. *Climate Dynamics*, *61*(1–2), 229–253. https://doi.org/10.1007/s00382-022-06565-x

González-Alemán, J. J., Insua-Costa, D., Bazile, E., González-Herrero, S., Marcello Miglietta, M., Groenemeijer, P., & Donat, M. G. (2023). Anthropogenic Warming Had a Crucial Role in Triggering the Historic and Destructive Mediterranean Derecho in Summer 2022. *Bulletin of the American Meteorological Society*, *104*(8), E1526–E1532. https://doi.org/10.1175/BAMS-D-23-0119.1

Guinaldo, T., Voldoire, A., Waldman, R., Saux Picart, S., & Roquet, H. (2023). Response of the sea surface temperature to heatwaves during the France 2022 meteorological summer. *Ocean Science*, *19*(3), 629–647. https://doi.org/10.5194/os-19-629-2023

Hersbach, H., Bell, B., Berrisford, P., Hirahara, S., Horányi, A., Muñoz-Sabater, J., Nicolas, J., Peubey, C., Radu, R., Schepers, D., Simmons, A., Soci, C., Abdalla, S., Abellan, X., Balsamo, G., Bechtold, P., Biavati, G., Bidlot, J., Bonavita, M., … Thépaut, J. (2020). The ERA5 global reanalysis. *Quarterly Journal of the Royal Meteorological Society*, *146*(730), 1999–2049. https://doi.org/10.1002/qj.3803

Jarvis, A., Reuter, H. I., Nelson, A., & Guevara, E. (2008). *Hole-filled seamless SRTM data V4, International Centre for Tropical Agriculture (CIAT)*. available from http://srtm.csi.cgiar.org.

Khodayar, S., Fosser, G., Berthou, S., Davolio, S., Drobinski, P., Ducrocq, V., Ferretti, R., Nuret, M., Pichelli, E., Richard, E., & Bock, O. (2016). A seamless weather–climate multi-model intercomparison on the representation of a high impact weather event in the western Mediterranean: <scp>HyMeX IOP12</scp>. *Quarterly Journal of the Royal Meteorological Society*, *142*(S1), 433–452. https://doi.org/10.1002/qj.2700

Kreitz, M. (2021). *Trois phénomènes météorologiques exceptionnels durant l'automne 2020*.

Krichak, S. O., Barkan, J., Breitgand, J. S., Gualdi, S., & Feldstein, S. B. (2015). The role of the export of tropical moisture into midlatitudes for extreme precipitation events in the Mediterranean region. *Theoretical and Applied Climatology*, *121*(3–4), 499–515. https://doi.org/10.1007/s00704-014-1244-6

Le Moigne, P., Besson, F., Martin, E., Boé, J., Boone, A., Decharme, B., Etchevers, P., Faroux, S., Habets, F., Lafaysse, M., Leroux, D., & Rousset-Regimbeau, F. (2020). The latest improvements with SURFEX v8.0 of the Safran–Isba–Modcou hydrometeorological model for France. *Geoscientific Model Development*, *13*(9), 3925–3946. https://doi.org/10.5194/gmd-13-3925-2020

Lebeaupin Brossier, C., Ducrocq, V., & Giordani, H. (2008). Sensitivity of three Mediterranean heavy rain events to two different sea surface fluxes parameterizations in high-resolution numerical modeling. *Journal of Geophysical Research: Atmospheres*, *113*(D21). https://doi.org/10.1029/2007JD009613

Lebeaupin, C., Ducrocq, V., & Giordani, H. (2006). Sensitivity of torrential rain events to the sea surface temperature based on high-resolution numerical forecasts. *Journal of Geophysical Research: Atmospheres*, *111*(D12). https://doi.org/10.1029/2005JD006541

Lucas-Picher, P., Brisson, E., Caillaud, C., Alias, A., Nabat, P., Lemonsu, A., Poncet, N., Cortés Hernandez, V. E., Michau, Y., Doury, A., Monteiro, D., & Somot, S. (2023). Evaluation of the convection-permitting regional climate model CNRM-AROME41t1 over Northwestern Europe. *Climate Dynamics*. https://doi.org/10.1007/s00382-022-06637-y

Lucas-Picher, P., Caya, D., Biner, S., & Laprise, R. (2008). Quantification of the Lateral Boundary Forcing of a Regional Climate Model Using an Aging Tracer. *Monthly Weather Review*, *136*(12), 4980–4996. https://doi.org/10.1175/2008MWR2448.1

Masson, V., Champeaux, J.-L., Chauvin, F., Meriguet, C., & Lacaze, R. (2003). A Global Database of Land Surface Parameters at 1-km Resolution in Meteorological and Climate Models. *Journal of Climate*, *16*(9), 1261–1282. https://doi.org/10.1175/1520-0442-16.9.1261

Masson, V., Le Moigne, P., Martin, E., Faroux, S., Alias, A., Alkama, R., Belamari, S., Barbu, A., Boone, A., Bouyssel, F., Brousseau, P., Brun, E., Calvet, J.-C., Carrer, D., Decharme, B., Delire, C., Donier, S., Essaouini, K., Gibelin, A.-L., … Voldoire, A. (2013). The SURFEXv7.2 land and ocean surface platform for coupled or offline simulation of earth surface variables and fluxes. *Geoscientific Model Development*, *6*(4), 929–960. https://doi.org/10.5194/gmd-6-929-2013

Matte, D., Laprise, R., Thériault, J. M., & Lucas-Picher, P. (2017). Spatial spin-up of fine scales in a regional climate model simulation driven by low-resolution boundary conditions. *Climate Dynamics*, *49*(1–2), 563–574. https://doi.org/10.1007/s00382-016-3358-2

Meredith, E. P., Semenov, V. A., Maraun, D., Park, W., & Chernokulsky, A. V. (2015). Crucial role of Black Sea warming in amplifying the 2012 Krymsk precipitation extreme. *Nature Geoscience*, *8*(8), 615–619. https://doi.org/10.1038/ngeo2483

Météo-France. (2021). *Tempête Alex du 2 octobre 2020*. http://tempetes.meteo.fr/IMG/anthemis_pdf/20201002.pdf

Nabat, P., Somot, S., Mallet, M., Chiapello, I., Morcrette, J. J., Solmon, F., Szopa, S., Dulac, F., Collins, W., Ghan, S., Horowitz, L. W., Lamarque, J. F., Lee, Y. H., Naik, V., Nagashima, T., Shindell, D., & Skeie, R. (2013). A 4-D climatology (1979–2009) of the monthly tropospheric aerosol optical depth distribution over the Mediterranean region from a comparative evaluation and blending of remote sensing and model products.

Atmospheric Measurement Techniques, *6*(5), 1287–1314. https://doi.org/10.5194/amt-6-1287-2013

Nuissier, O., Ducrocq, V., Ricard, D., Lebeaupin, C., & Anquetin, S. (2008). A numerical study of three catastrophic precipitating events over southern France. I: Numerical framework and synoptic ingredients. *Quarterly Journal of the Royal Meteorological Society*, *134*(630), 111–130. https://doi.org/10.1002/qj.200

Payrastre, O., Nicolle, P., Bonnifait, L., Brigode, P., Astagneau, P., Baise, A., Belleville, A., Bouamara, N., Bourgin, F., Breil, P., Brunet, P., Cerbelaud, A., Courapied, F., Devreux, L., Dreyfus, R., Gaume, E., Nomis, S., Poggio, J., Pons, F., … Sevrez, D. (2022). Tempête Alex du 2 octobre 2020 dans les Alpes-Maritimes : une contribution de la communauté scientifique à l'estimation des débits de pointe des crues. *LHB*, *108*(1). https://doi.org/10.1080/27678490.2022.2082891

Pfahl, S., O'Gorman, P. A., & Fischer, E. M. (2017). Understanding the regional pattern of projected future changes in extreme precipitation. *Nature Climate Change*, *7*(May), 423–428. https://doi.org/10.1038/nclimate3287

Pichelli, E., Coppola, E., Sobolowski, S., Ban, N., Giorgi, F., Stocchi, P., Alias, A., Belušić, D., Berthou, S., Caillaud, C., Cardoso, R. M., Chan, S., Christensen, O. B., Dobler, A., de Vries, H., Goergen, K., Kendon, E. J., Keuler, K., Lenderink, G., … Vergara-Temprado, J. (2021). The first multi-model ensemble of regional climate simulations at kilometer-scale resolution part 2: historical and future simulations of precipitation. *Climate Dynamics*. https://doi.org/10.1007/s00382-021-05657-4

Prein, A. F., Langhans, W., Fosser, G., Ferrone, A., Ban, N., Goergen, K., Keller, M., Tölle, M., Gutjahr, O., Feser, F., Brisson, E., Kollet, S., Schmidli, J., Van Lipzig, N. P. M., & Leung, R. (2015). A review on regional convection-permitting climate modeling: Demonstrations, prospects, and challenges. In *Reviews of Geophysics* (Vol. 53, Issue 2, pp. 323–361). Blackwell Publishing Ltd. https://doi.org/10.1002/2014RG000475

Rainaud, R., Brossier, C. L., Ducrocq, V., & Giordani, H. (2017). High-resolution air–sea coupling impact on two heavy precipitation events in the Western Mediterranean. *Quarterly Journal of the Royal Meteorological Society*, *143*(707), 2448–2462. https://doi.org/10.1002/qj.3098

Ribes, A., Boé, J., Qasmi, S., Dubuisson, B., Douville, H., & Terray, L. (2022). An updated assessment of past and future warming over France based on a regional observational constraint. *Earth System Dynamics*, *13*(4), 1397–1415. https://doi.org/10.5194/esd-13-1397-2022

Ribes, A., Thao, S., Vautard, R., Dubuisson, B., Somot, S., Colin, J., Planton, S., & Soubeyroux, J. M. (2019). Observed increase in extreme daily rainfall in the French Mediterranean. *Climate Dynamics*, *52*(1–2), 1095–1114. https://doi.org/10.1007/s00382-018-4179-2

Seity, Y., Brousseau, P., Malardel, S., Hello, G., Bénard, P., Bouttier, F., Lac, C., & Masson, V. (2011). The AROME-France Convective-Scale Operational Model. *Monthly Weather Review*, *139*(3), 976–991. https://doi.org/10.1175/2010MWR3425.1

Simon, A., Pires, C., Frölicher, T. L., & Russo, A. (2023). Long-term warming and interannual variability contributions' to marine heatwaves in the Mediterranean. *Weather and Climate Extremes*, *42*, 100619. https://doi.org/10.1016/j.wace.2023.100619

van Vuuren, D. P., Edmonds, J., Kainuma, M., Riahi, K., Thomson, A., Hibbard, K., Hurtt, G. C., Kram, T., Krey, V., Lamarque, J. F., Masui, T., Meinshausen, M., Nakicenovic, N., Smith, S. J., & Rose, S. K. (2011). The representative concentration pathways: An overview. *Climatic Change*, *109*(1), 5–31. https://doi.org/10.1007/s10584-011-0148-z

Acknowledgements

We thank Edith Cortés for post-processing the observed orography.

Statements & Declarations

Funding. This project has received funding from the European Union's Horizon 2020 research and innovation programme under the Marie Sklodowska-Curie grant agreement No 101027577".

Competing interests. The authors declare they have no financial interests.

Author contributions. All authors contributed to the study conception and design. Material preparation, data collection and analysis were performed by MB, with the help of MPM, CC, and AA to carry out the simulations with CNRM-AROME. JB, LT and CC helped designing the modeling experiments and contributed to the interpretation of the results. The first draft of the manuscript was written by MB and all authors commented on previous versions of the manuscript. All authors read and approved the final manuscript.

Data availability. The simulations produced for this research can be made available from the corresponding author on reasonable request. The COMEPHORE observations will be made freely available from the Meteo-France institute throughout the year 2024.

Figures

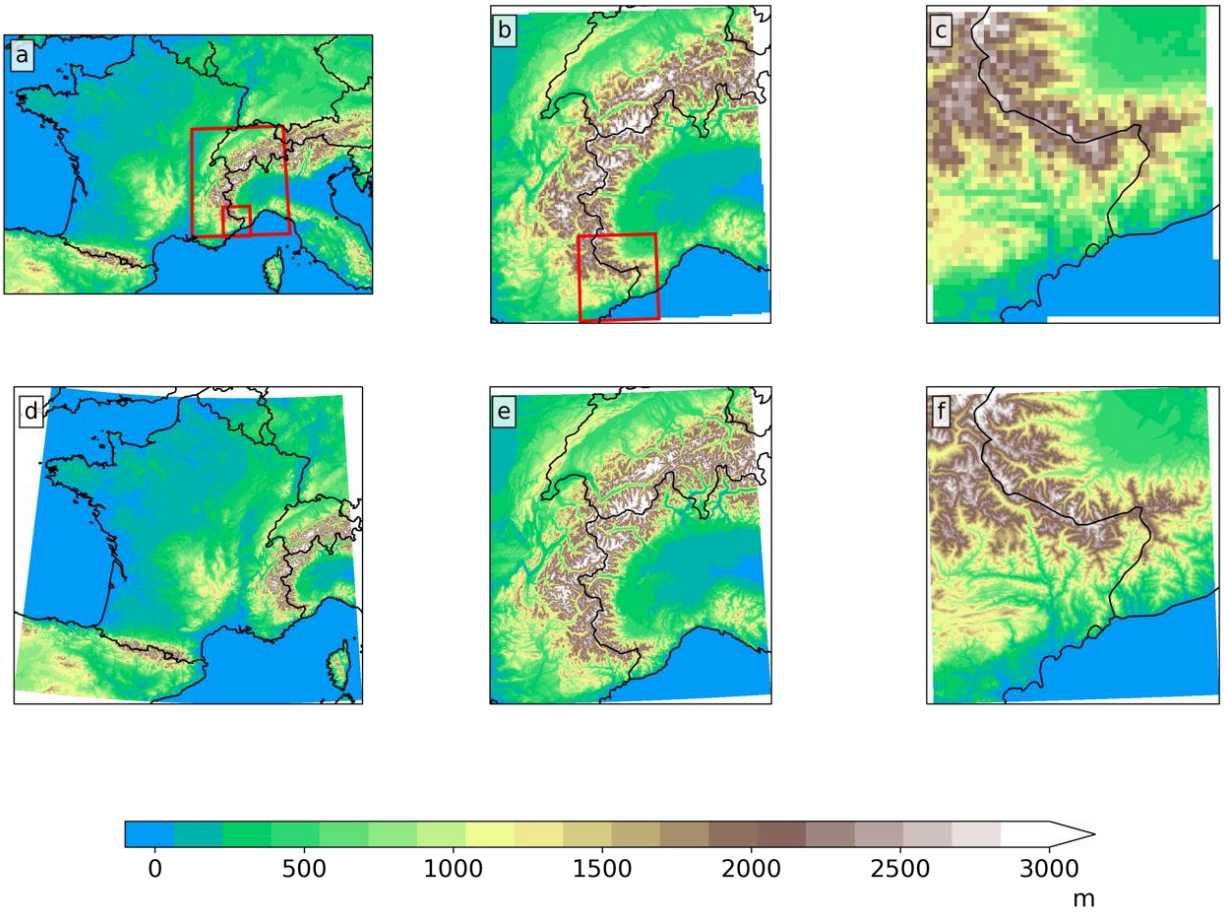

Figure 1: Orography (in m) in CNRM-AROME (top) and in pseudo-observations (bottom) over the three domains used in this study: the entire domain (left), an intermediate domain covering the western Alps (middle), and a smaller region centered over the French Alpes-Maritimes region (right). The intermediate and smaller region are also indicated by the red boxes on panels (a) and (b).

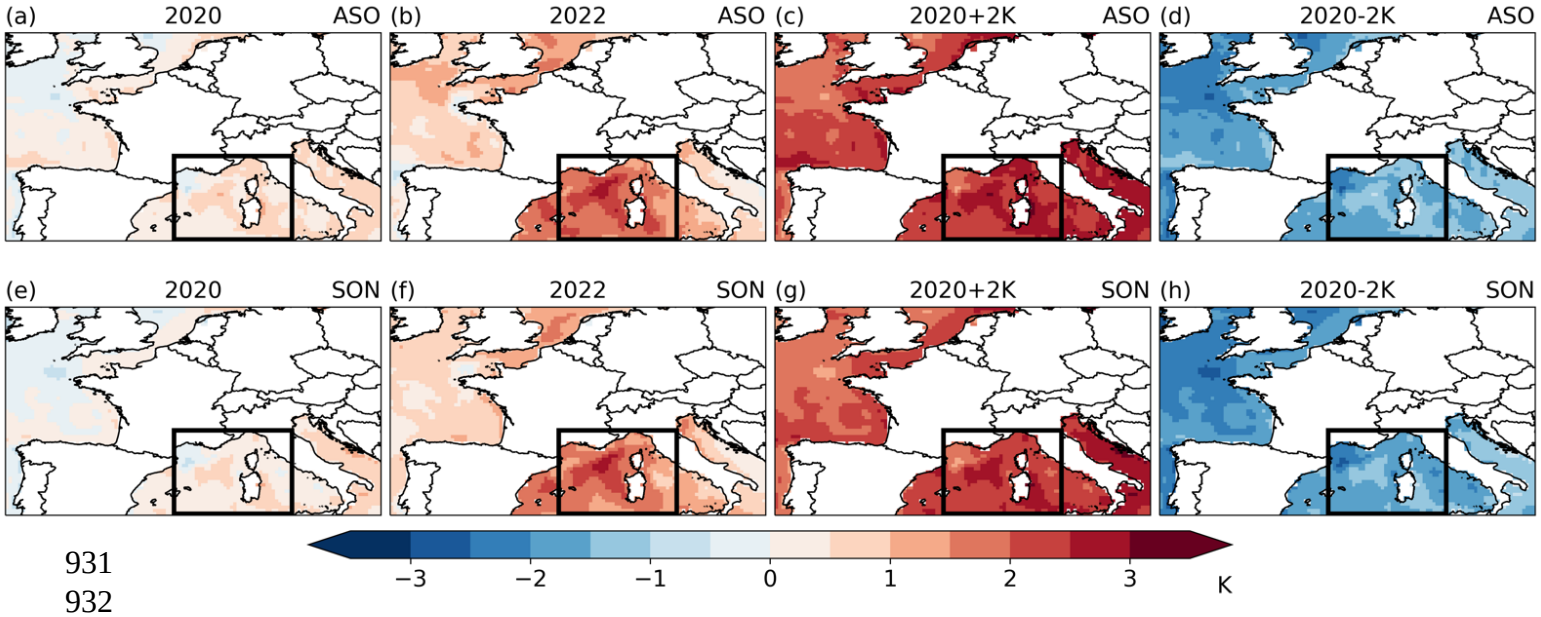

Figure 2: Mean August-September-October (ASO; top) and September-October-November (SON; bottom) sea surface temperature anomalies (in K) to the 1993-2022 climatology in the ERA5 reanalysis for the years 2020 (a,e), 2022 (b,d), and for the idealized anomalies of the year 2020 with the addition of uniform 2K warming (c,g) and cooling (d,h).

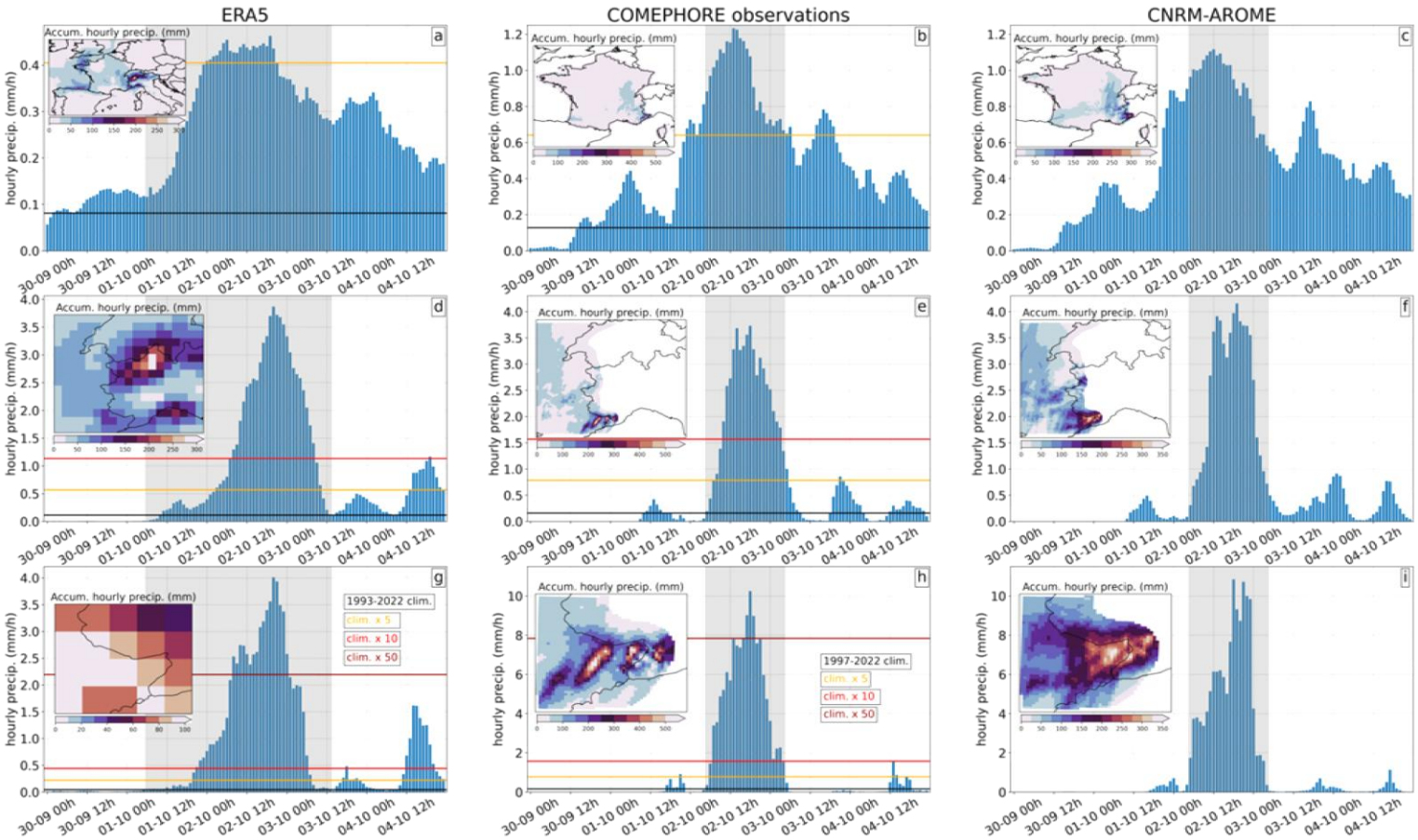

939 **Figure 3:** Hourly evolution of precipitation (in mm) averaged over the domains depicted in
940 the inserted maps on each individual panels, from September 30 to October 4, 2020, in (left)
941 the ERA5 reanalysis, (middle) the COMEPHORE observations, and (right) the *CTRL* ensemble
942 mean of the CNRM-AROME model. Inserted maps show the accumulated hourly
943 precipitation over the time window indicated by the grey shading on each individual panel.
944 The three domains (per row) correspond to the different domains investigated in this study
945 (see section 2.5). ERA5 data is at the native 25 km resolution, while COMEPHORE and
946 CNRM-AROME data are at a resolution of 2.5 km, and the spatial coverage is constrained to
947 match those of the observations.. Horizontal colored lines for ERA5 and COMEPHORE data
948 represent exceeding levels (see inserted legends) of precipitation intensity relative to their
949 5-day climatology (September 30 to October 4; 1993-2022 period for ERA5 and 1997-2020
950 period for COMEPHORE).

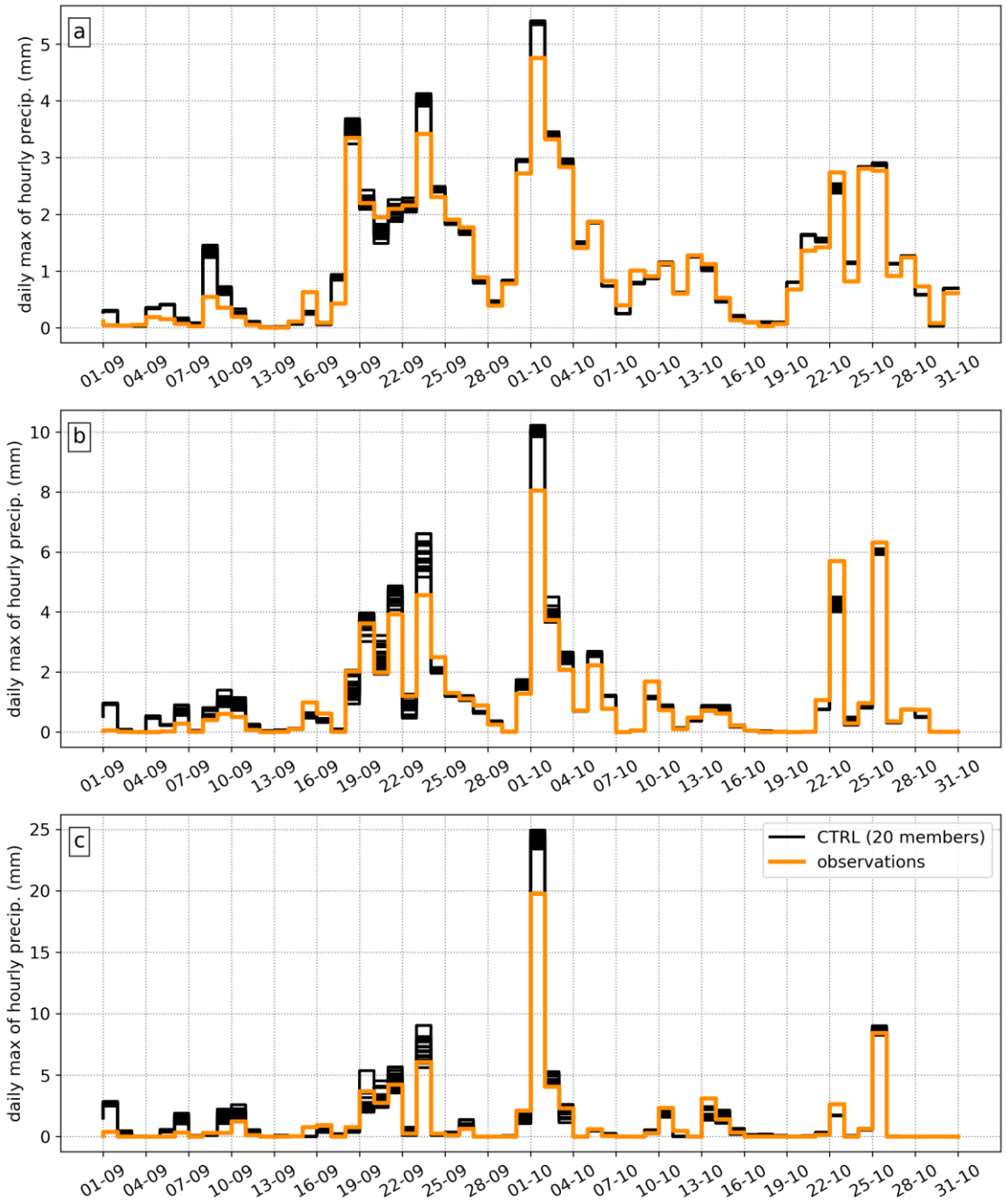

Figure 4: Observed (orange) and simulated (black; in the 20 members of the *CTRL* ensemble) daily maxima of hourly precipitation (in mm) averaged over (a) the entire domain, (b) the intermediate domain of the western Alps, and (c) the smaller region of the French Alpes-Maritimes. The COMEPHORE observations and CNRM-AROME data are at a resolution of 2.5 km, and the spatial coverage is constrained to match those of the observations.

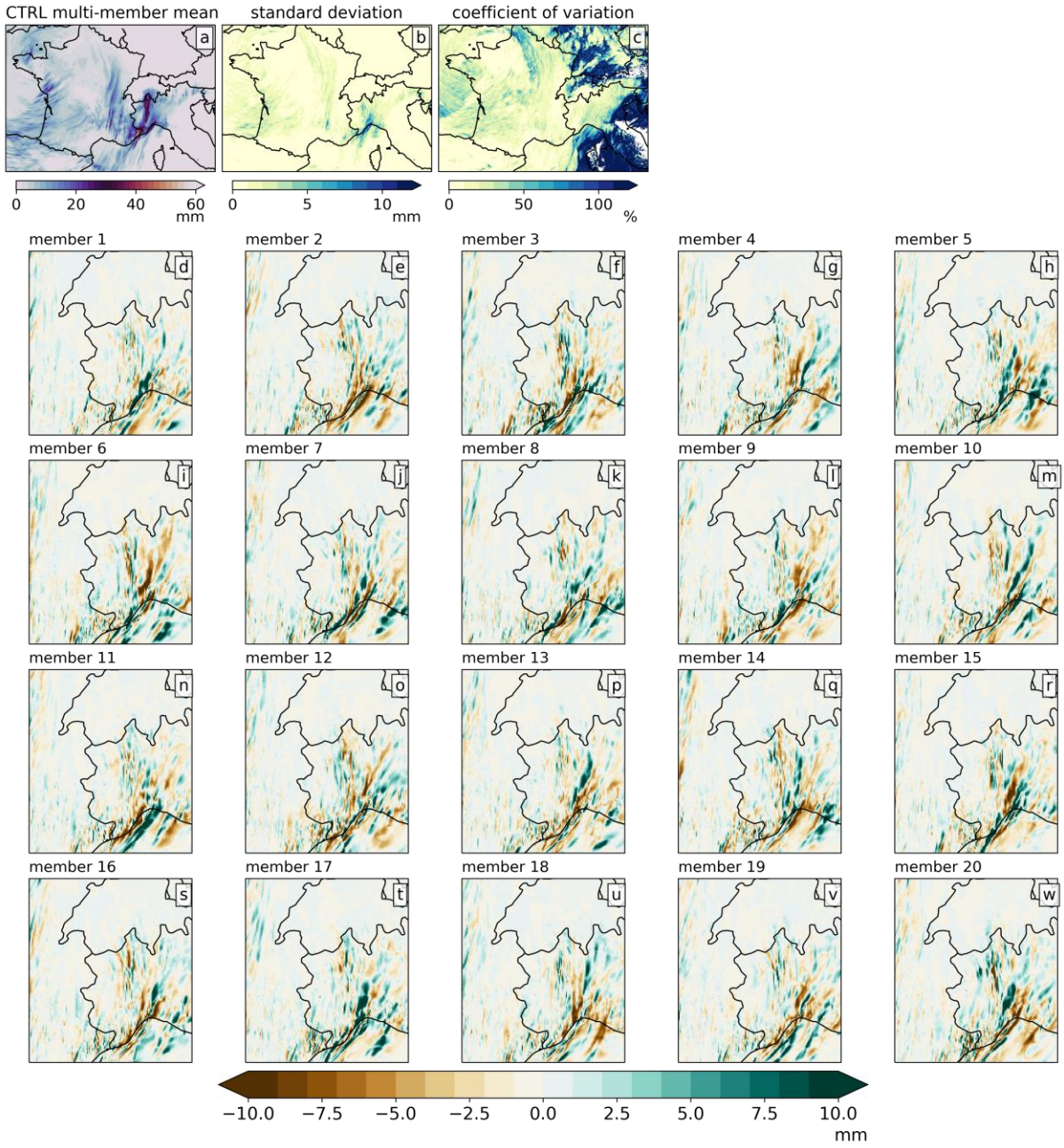

Figure 5: Maximum of hourly precipitation on October 2 in the *CTRL* multi-member mean (a; in mm) and its corresponding standard deviation (b; in mm) and coefficient of variation (c; standard deviation normalized by the climatology, in %). Panels d-w show the difference to the CTRL ensemble mean for each of the 20 members of the *CTRL* experiment (in mm).

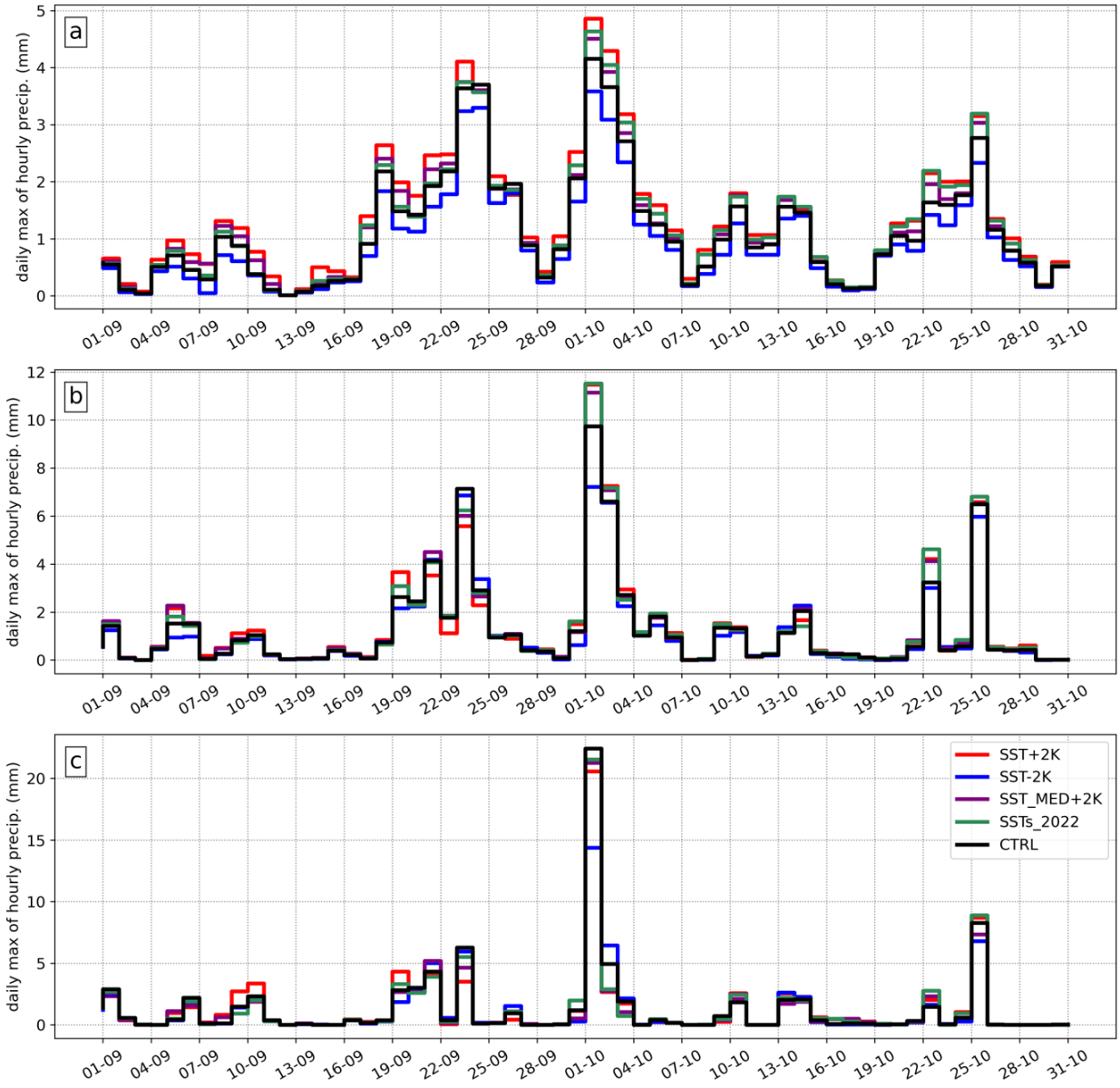

Figure 6: Daily maxima of hourly precipitation (in mm) in the ensemble mean of the different modeling experiments (see inserted legend) averaged over (a) the entire domain, (b) the intermediate domain of the western Alps, and (c) the smaller region of the French Alpes-Maritimes.

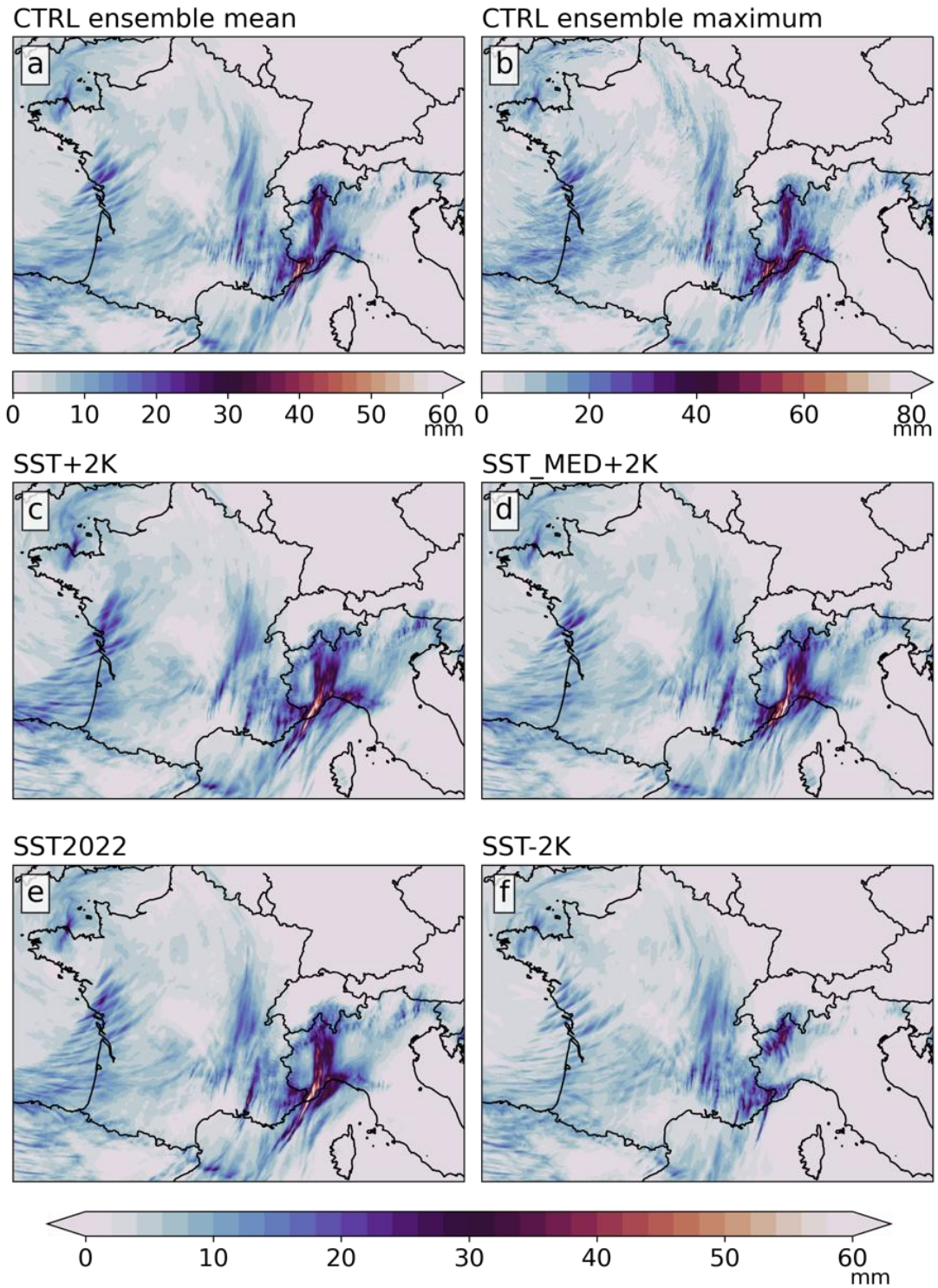

Figure 7: Maximum of hourly precipitation (in mm) on October 2 in the ensemble mean of the following modeling experiments: (a) CTRL, (c) SST+2K, (d) SST_MED+2K, (e) SST2022, and (f) SST-2K. Panel (b) displays the maximum value (in mm) across the 20 members of *CTRL*.

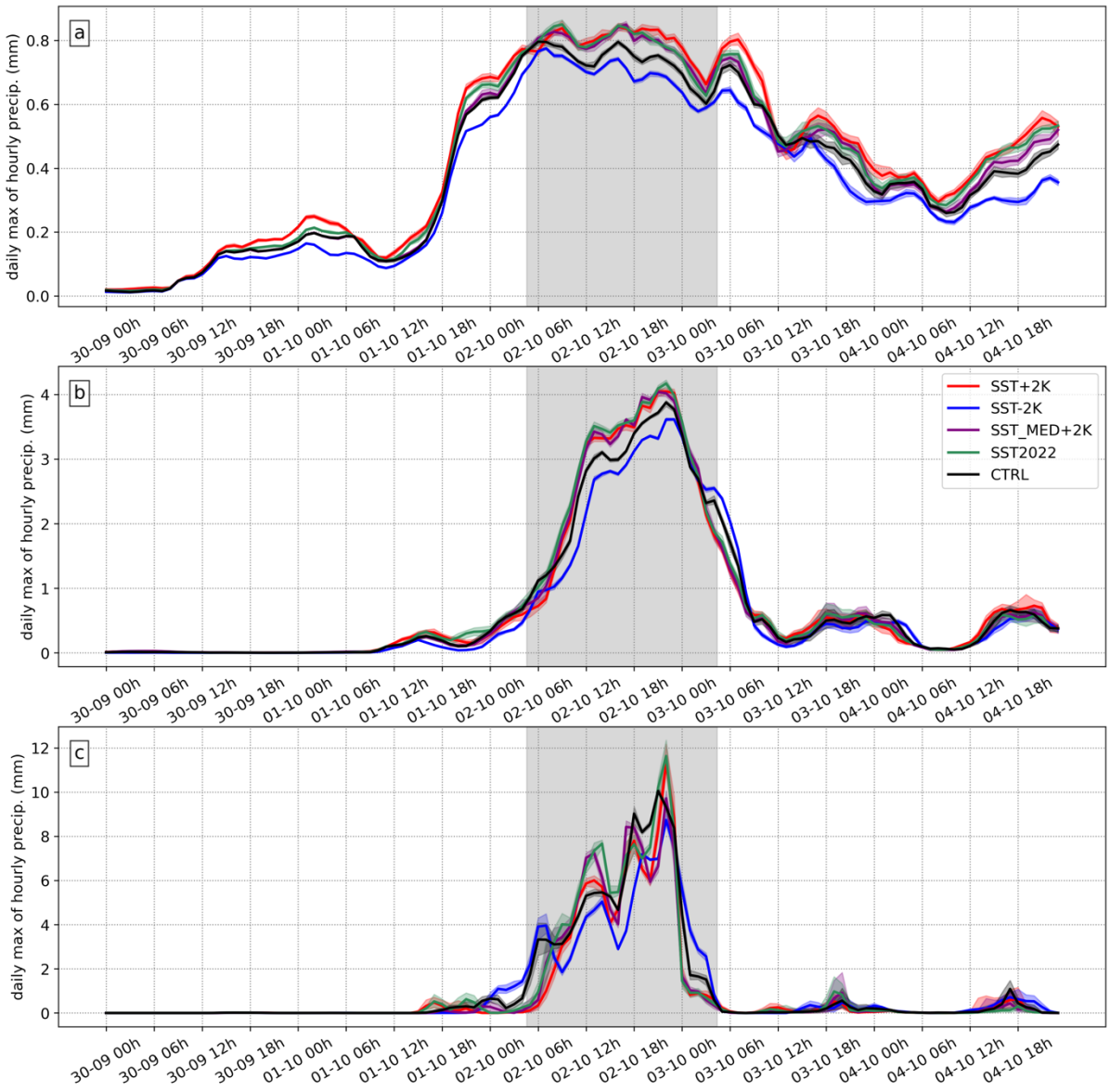

Figure 8: Hourly evolution of precipitation (in mm) over the 5-day period from September 30 to October 4, 2020, averaged over (a) the entire domain, (b) the intermediate domain of the western Alps, and (c) the smaller region of the French Alpes-Maritimes. The five modeling experiments conducted with CNRM-AROME are shown using the color-code provided in the inserted legend. For each experiment, the ensemble mean is represented by the thick line, and the respective shading indicates the minimum-maximum range across the 20 members. The grey shading corresponds the 24-hour time window that best captures the 2020 Mediterranean HPE and is used in Figures 9 to 13.

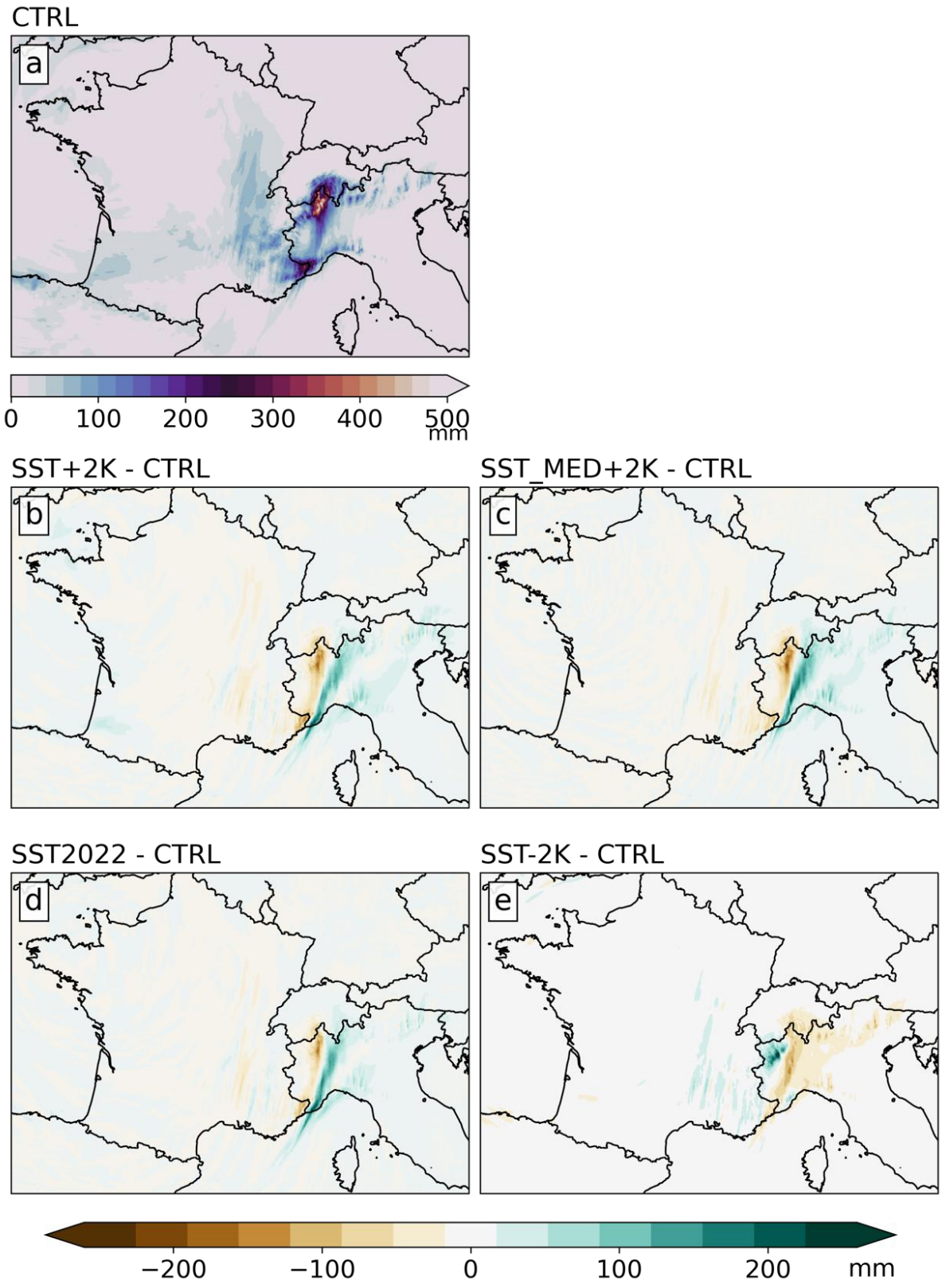

Figure 9: Accumulated precipitation (in mm) over the 24-hour period that best captures the 2020 Mediterranean HPE (refer to grey shading in Figure 8) in (a) the *CTRL* ensemble mean, and the difference to the *CTRL* ensemble mean for the (b) *SST+2K*, (c) *SST_MED+2K*, (d) *SST2022* and (e) *SST-2K* ensemble mean.

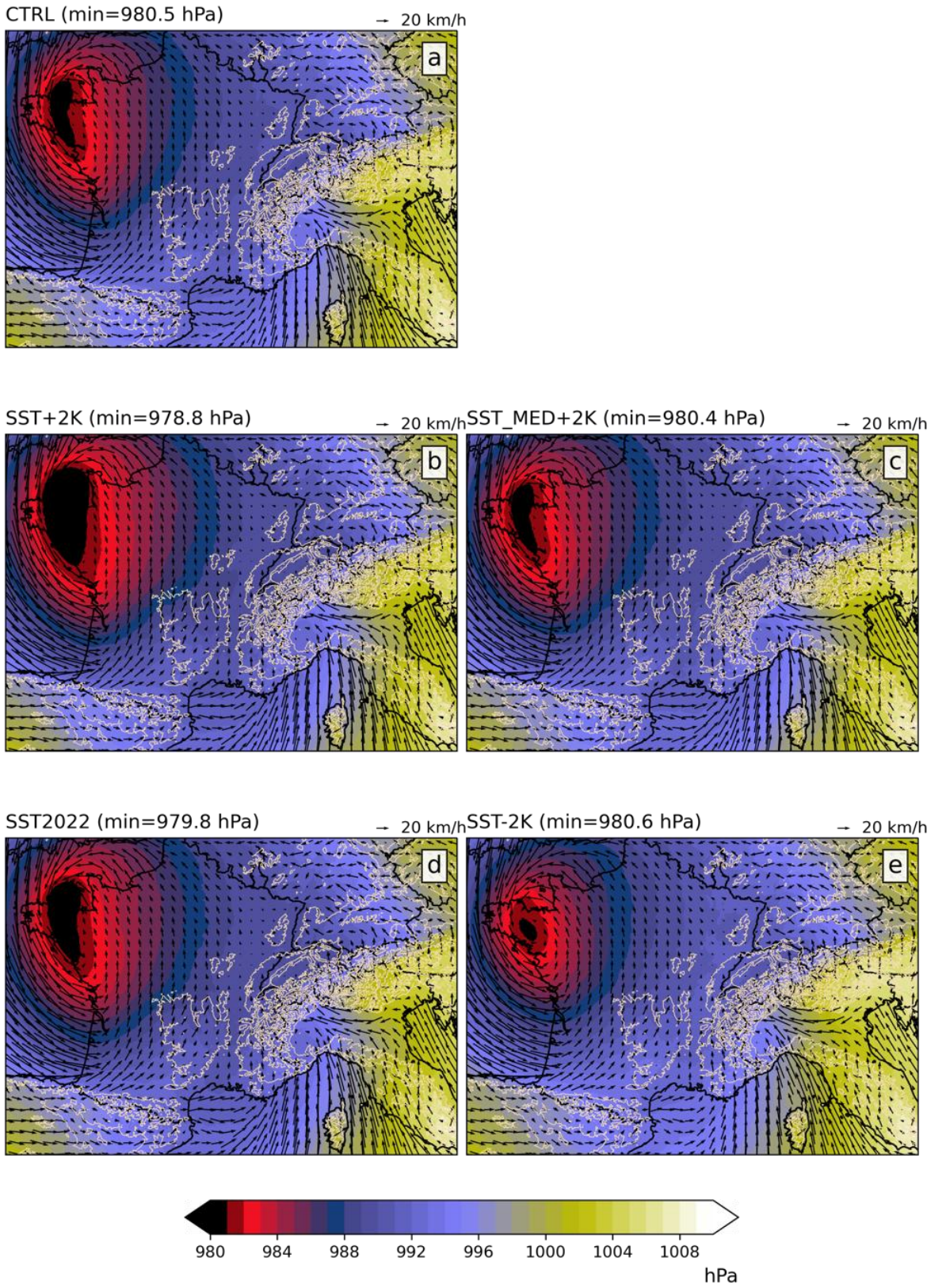

Figure 10: Mean sea level pressure (contours; in hPa) and surface winds (vectors; in km/h) over the 24-hour period that best captures the 2020 Mediterranean HPE (refer to grey shading in Figure 8) in the ensemble mean of the (a) *CTRL*, (b) *SST+2K*, (c) *SST_MED+2K*, (d) *SST2022*, and (e) *SST-2K* experiment. The minimum sea level pressure value over the domain is indicated at the top of each panel. Orography is represented by the white contours at the 500, 1500, and 2500 m levels.

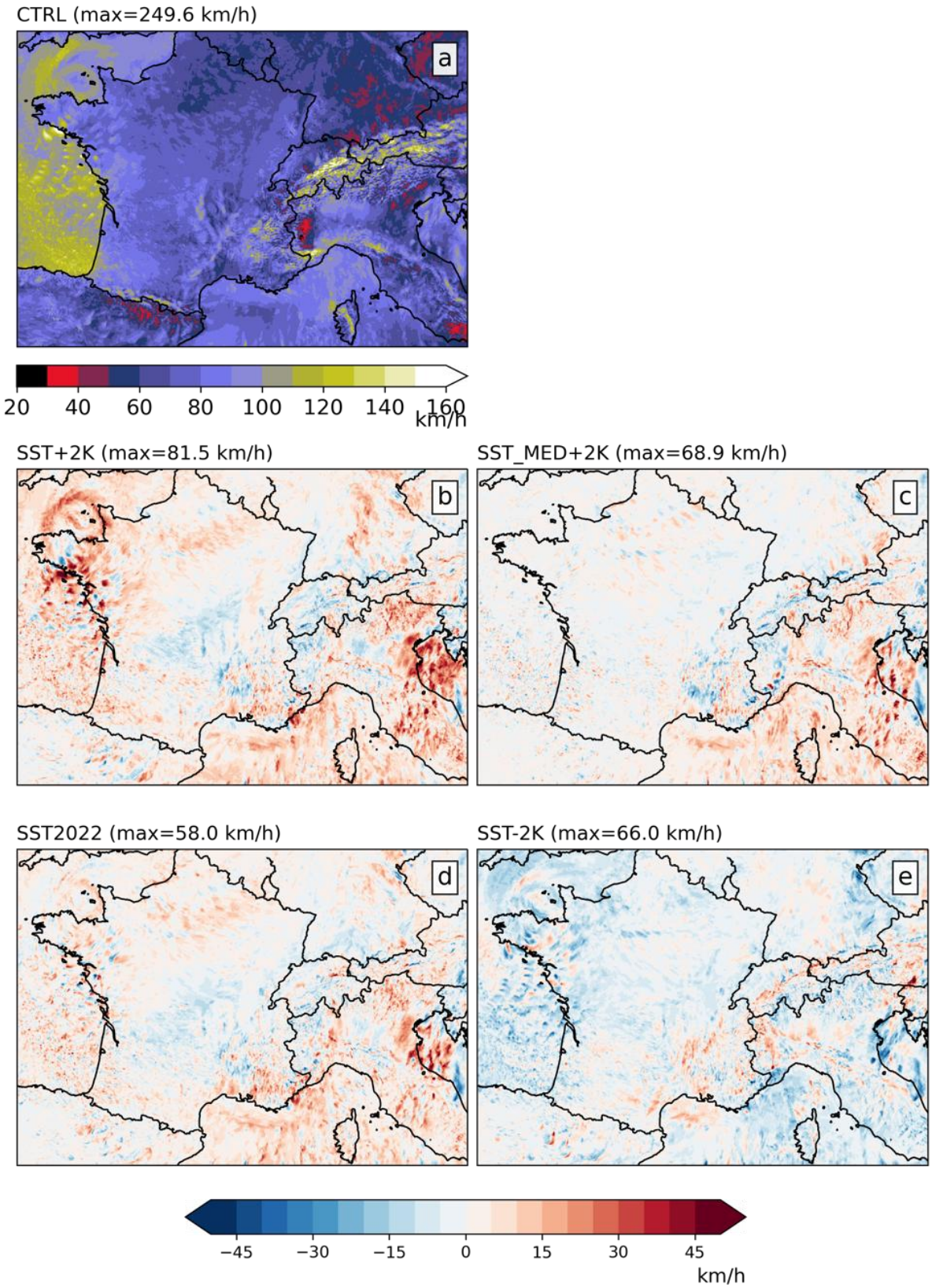

Figure 11: Mean daily maximum near-surface wind speed of gust (in km/h) over the 24-hour period that best captures the 2020 Mediterranean HPE (refer to grey shading in Figure 8) in (a) the *CTRL* ensemble mean, and the difference to the *CTRL* ensemble mean for the (b) *SST+2K*, (c) *SST_MED+2K*, (d) *SST2022* and (e) *SST-2K* ensemble mean. The maximum value over the domain is indicated at the top of each panel.

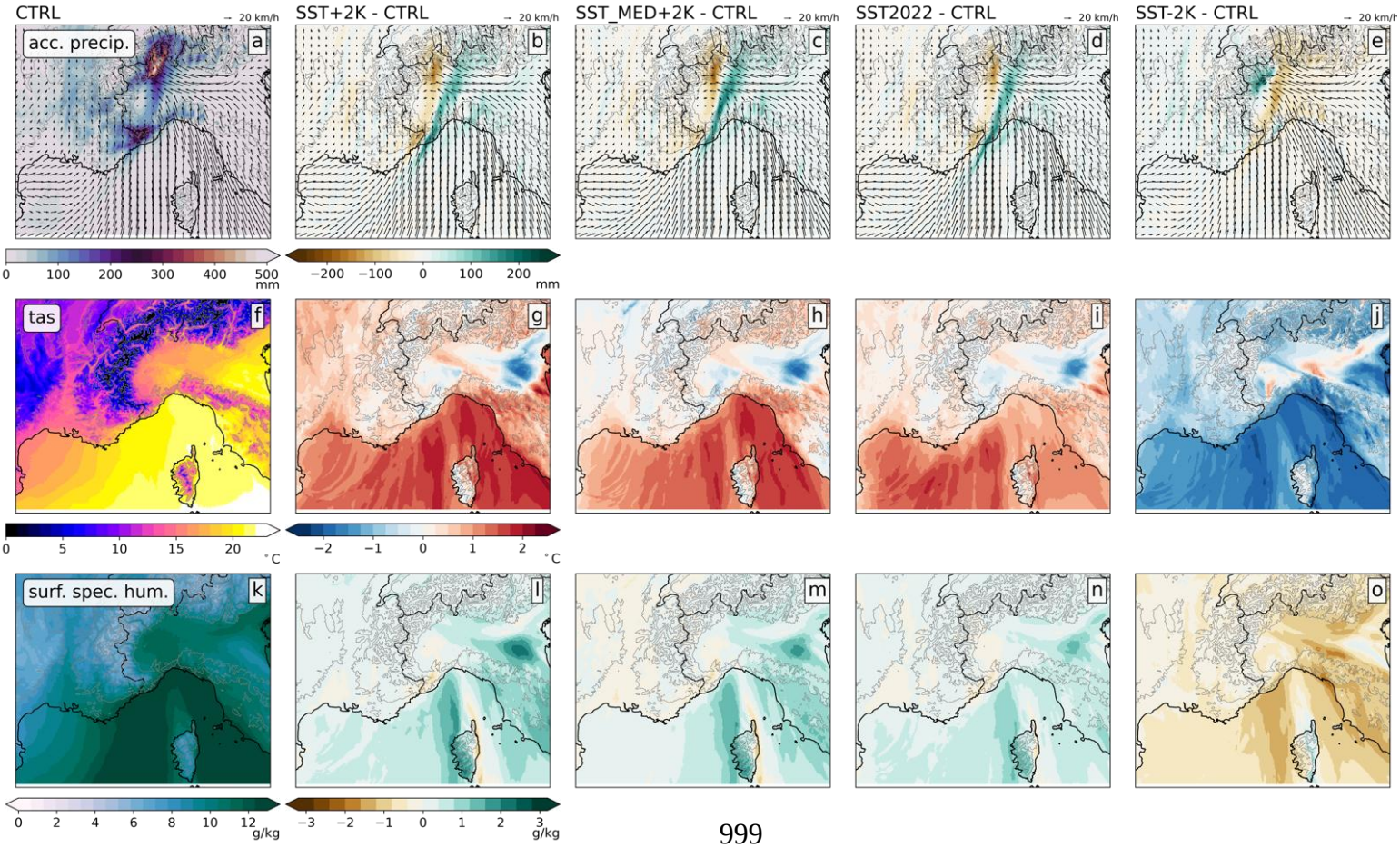

Figure 12: Mean accumulated precipitation (contours; in mm) and surface winds (vectors; in km/h) (first row), surface air temperature (in °C; second row), and surface specific humidity (in g/kg; third row) over the 24-hour period that best captures the 2020 Mediterranean HPE (refer to grey shading in Figure 8) in (a,f,k) the *CTRL* ensemble mean, and the difference to the *CTRL* ensemble mean for the (b,g,l) *SST+2K*, (c,h,m) *SST_MED+2K*, (d,I,n) *SST2022* and (e,j,o) *SST-2K* ensemble mean.

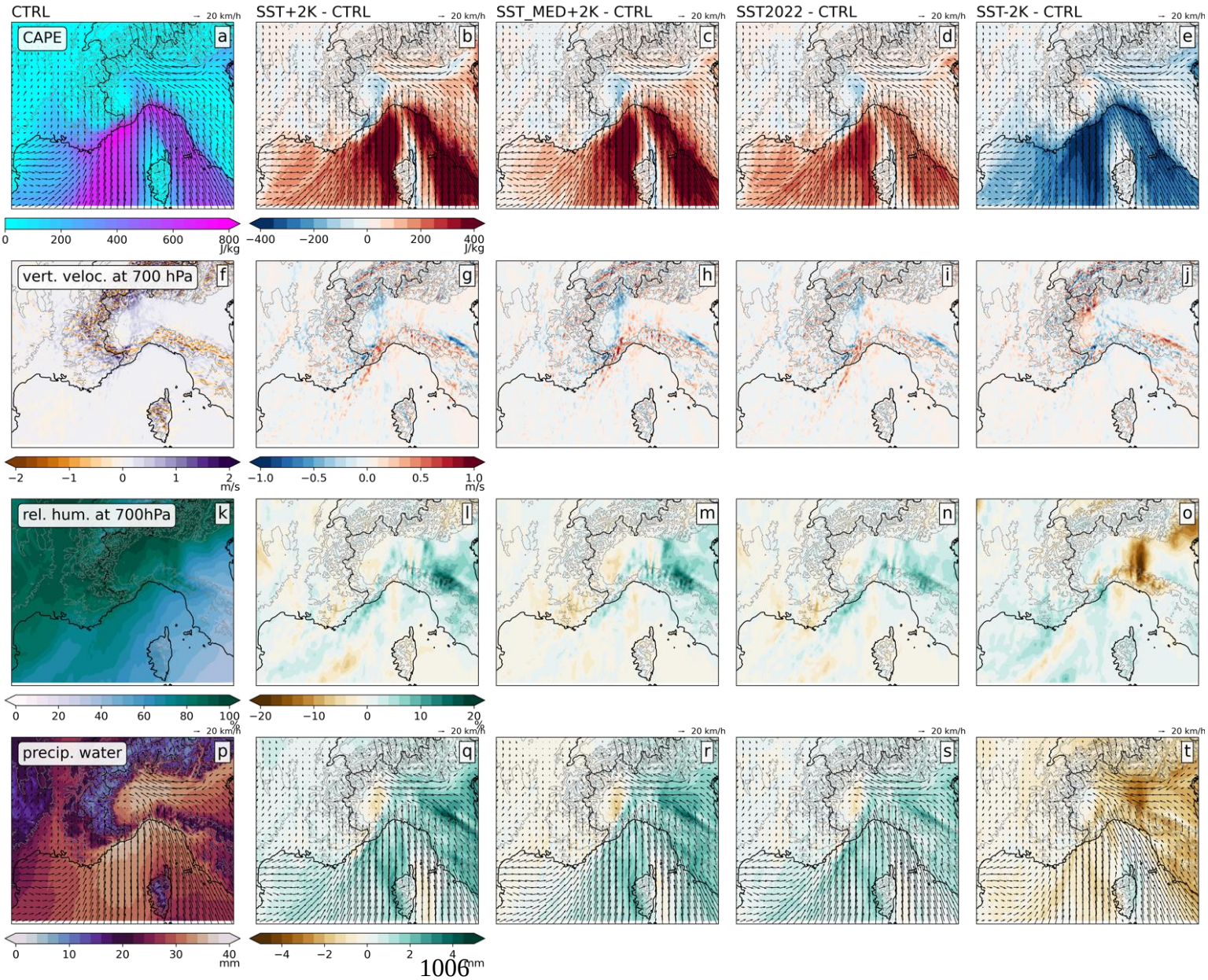

1006

1007 **Figure 13:** Mean CAPE (contours; in J/kg) and surface winds (vectors; in km/h) (first row),
1008 vertical velocity at 700 hPa (in m/s; second row), relative humidity at 700 hPa (in %; third
1009 row), and precipitable water (contours; in mm) and surface winds (vectors; in km/h) (fourth
1010 row) over the 24-hour period that best captures the 2020 Mediterranean HPE (refer to grey
1011 shading in Figure 8) in (a,f,k,p) the *CTRL* ensemble mean, and the difference to the *CTRL*
1012 ensemble mean for the (b,g,l,q) *SST+2K*, (c,h,m,r) *SST_MED+2K*, (d,I,n,s) *SST2022* and (e,j,o,t)
1013 *SST-2K* ensemble mean.